UNITED NATIONS UNIVERSITY

UNU-GTP

ORKUSTOFNUN

Meyjarauga hot spring, Hveravellir, Kjölur, Central Iceland

Hamoud Souleiman Cheik

FEASIBILITY STUDY FOR IMPLEMENTATION OF A BINARY POWER PLANT IN LAKE ABHÉ GEOTHERMAL AREA WITH A PARTICULAR HOT ARID CLIMATE, DJIBOUTI

Report 3
November 2018

UNITED NATIONS UNIVERSITY
UNU-GTP
Geothermal Training Programme

Orkustofnun, Grensasvegur 9,
IS-108 Reykjavik, Iceland

Reports 2018
Number 3

FEASIBILITY STUDY FOR IMPLEMENTATION OF A BINARY POWER PLANT IN LAKE ABHÉ GEOTHERMAL AREA WITH A PARTICULAR HOT ARID CLIMATE, DJIBOUTI

MSc Thesis
Master of Science in Sustainable Energy Engineering
Iceland School of Energy
Reykjavik University

by

Hamoud Souleiman Cheik
Ministry of Energy and Water in Charge of Natural Resources
P.O. Box 10010
Djibouti
DJIBOUTI
hamoudsoulei@yahoo.fr

United Nations University
Geothermal Training Programme
Reykjavík, Iceland
Published in November 2018

ISBN 978-9979-68-481-7 (PRINT)
ISBN 978-9979-68-482-4 (PDF)
ISSN 1670-7427

This MSc thesis has also been published in May 2018 by the
Iceland School of Energy
Reykjavík University

INTRODUCTION

The Geothermal Training Programme of the United Nations University (UNU) has operated in Iceland since 1979 with six-month annual courses for professionals from developing countries. The aim is to assist developing countries with significant geothermal potential to build up groups of specialists that cover most aspects of geothermal exploration and development. During 1979-2018, 694 scientists and engineers from 61 developing countries have completed the six month courses, or similar. They have come from Africa (39%), Asia (35%), Latin America (14%), Europe (11%), and Oceania (1%). There is a steady flow of requests from all over the world for the six-month training and we can only meet a portion of the requests. Most of the trainees are awarded UNU Fellowships financed by the Government of Iceland.

Candidates for the six-month specialized training must have at least a BSc degree and a minimum of one-year practical experience in geothermal work in their home countries prior to the training. Many of our trainees have already completed their MSc or PhD degrees when they come to Iceland, but many excellent students with only BSc degrees have made requests to come again to Iceland for a higher academic degree. From 1999, UNU Fellows have also been given the chance to continue their studies and study for MSc degrees in geothermal science or engineering in co-operation with the University of Iceland. An agreement to this effect was signed with the University of Iceland. A similar agreement was also signed with Reykjavik University in 2013. The six-month studies at the UNU Geothermal Training Programme form a part of the graduate programme.

It is a pleasure to introduce the 59th UNU Fellow to complete the MSc studies under a UNU-GTP Fellowship. Hamoud Souleiman Cheik, Electrical Engineer from the Ministry of Energy and Water in Charge of Natural Resources, Republic of Djibouti, completed the six-month specialized training in *Geothermal Utilization* at UNU Geothermal Training Programme in October 2010. His research report was entitled: *Prefeasibility design of a 2×25 MW single-flash geothermal power plant in Asal, Djibouti.* After six years of geothermal work for the Ministry of Energy and Water in Charge of Natural Resources in Djibouti, he came back to Iceland for MSc studies at Iceland School of Energy, Reykjavik University in July 2016. In April 2018, he defended his MSc thesis in Sustainable Energy Engineering presented here, entitled: *Feasibility study for implementation of a binary power plant in Lake Abhé geothermal area with a particular hot arid climate, Djibouti*. His studies in Iceland were financed by the Government of Iceland through a UNU-GTP Fellowship from the UNU Geothermal Training Programme. We congratulate Hamoud on the achievements and wish him all the best for the future. We thank Iceland School of Energy, Reykjavik University, for the co-operation, and his supervisors for the dedication.

Finally, I would like to mention that Hamoud's MSc thesis with the figures in colour is available for downloading on our website *www.unugtp.is*, under publications.

With warmest greetings from Iceland,

Lúdvík S. Georgsson, Director
United Nations University
Geothermal Training Programme

ACKNOWLEDGEMENTS

I am grateful to the Almighty Allah for sustaining me during the entire time of my study and stay in Iceland.

I wish to express my sincere gratitude to the United Nations University Geothermal Training Program (UNU-GTP) and Djiboutian Office for Development of Geothermal Energy (ODDEG) for giving me the opportunity to do my MSc in Sustainable Energy Engineering in Reykjavik University.

My gratitude goes to UNU-GTP staff: Director, Lúdvík S. Georgsson, Deputy Director, Ingimar G. Haraldsson, Service Manager, Markús A. G. Wilde, School Manager, Thórhildur Ísberg, and Environmental Scientist/Editor, Málfrídur Ómardóttir, for their guidance, assistance and care.

My special thanks go to my supervisor, Dr. María Sigrídur Gudjónsdóttir, assistant professor at Reykjavik University, for her dedicated support and guidance during project preparation, research and writing, which made it possible for me to complete this report.

Last but not least, I am grateful to my family for their endurance, emotional support, prayers, and encouragement during my study time in Iceland.

DEDICATION

To my Father, Souleiman Cheik Moussa

ABSTRACT

Lake Abhe, situated in Southwestern part of Djibouti is one of promising geothermal field and was recently the subject of a complete surface exploration. Located in a hot arid climatic zone, Djibouti possesses several medium-enthalpy resources distributed in different parts of the country. This particular climate makes it necessary to find new ways in modelling common geothermal power plants. The objective here is to determine how the medium-enthalpy resource in Lake Abhe geothermal field would be best utilized, both technically and commercially. The backbone of this paper will be how to deal with the hot, arid climate in order to maximize the net power output of the plant. A thermodynamic model was developed using Engineering Equation Solver (EES) to evaluate the performance of ORC geothermal power plants standalone with different cooling system, and an ORC assisted by a parabolic trough solar concentrating collector field. The water cooled condenser got 6,1% of the net power output more than the air cooled condenser (ACC) and was found to have more negative effects on the environment. Water usage was calculated to be 1324 kg/s or 41.8 million tons per year corresponding 1.4 % of the total lake water. This system draws energy out of the working fluid before expelling the water back into the Lake Abhe with an increase in water temperature of 17°C. The ACC and hybrid solar-geothermal designs were selected and the NPV and IRR of these designs were modelled to allow an economic comparison. This study estimates a geothermal fluid mass flow of 443 kg/s and temperature of 145.7°C. Under Djiboutian climatic conditions with an average ambient temperature of 30.04°C, the air-cooled condenser basic binary model produces 10,924 kWe of gross power output with an auxiliary power consumption of 22.6% of the total gross output power. The fan power represents 51.8% of the parasitic power. The cycle efficiency of the ACC is 10.44%. For the hybrid solar-geothermal power plant, the net power output is 13,865 kWe with 20.6% for the use of the auxiliary components. The cycle efficiency of the hybrid is 10.18%. The hybrid system shows higher power output (up to 21.24% difference) compared to ACC. This study finds the hybrid system to be a better option than individual geothermal system at all ambient temperatures. It is demonstrated that the hybrid is the most economically attractive scenario, providing the highest NPV of US $9,900,000 and the fastest payback period of 18 years with the highest IRR of 13%.

TABLE OF CONTENTS

LIST OF FIGURES

LIST OF TABLES

Page

1. INTRODUCTION

1.1 General overview of Djibouti Republic

The Republic of Djibouti is located in East horn of Africa. It is bordered by Ethiopia in the west and south, Eretria in the north, and Somalia in the southeast. It is hence a strategic place between Africa and Arabia the entrance of the Red Sea in the extreme West of the Aden Gulf, between latitudes 10° and 13°N and longitudes 41° and 44°E, within the Arabian Plate see Figure 1. With a total area of 23,200 km2, the current population of the Djibouti Republic is estimated to be about 850,000, of which about 600,000 live in the main town of Djibouti-Ville, 95,000 in secondary towns and the remainder, 155,000, in a rural setting, including a substantial nomadic population (DISED, 2009) (Souleiman and Moussa, 2015).

FIGURE 1: Map of Djibouti (Lonely Planet, 2018)

Situated on a strategically location the roundabout of three continent Asia, Africa and Europe, Djibouti is on major international shipping routes. The Republic of Djibouti is a regional transport hub. For Ethiopia, great with their 90 million inhabitants, Djibouti is presently the only access to the sea. The transport sector remains the mainstay of the national economy: port services and transit and road services are the main activities of the trade sector, which contributes over 70% to the creation of wealth. It has benefited in recent years from foreign direct investment in harbours, tourism and construction. Djibouti shelters in its land various foreign military camp such as France, USA, China, Italia, Japan as well as other countries.

1.2 Climate in Djibouti

Djibouti climate is classified as hot and arid. There are two seasons in Djibouti, the cold season starting from October to April and the hot season from May to September. The mean annual temperature at Djibouti-Ville is 30°C and occasional temperatures of 48°C have been recorded near Lake Asal (155 m b.s.l) (Hughes and Hughes, 1992). Total annual precipitation averages 163 mm, which is equivalent to 163.5 L/m^2. The lowest monthly relative humidity is 43% in July and the maximum appear in April and attain 74%. The average annual relative humidity is 63.3% (Climatemps, 2018). Humidity is always high at the coast but decreases dramatically in passing inland. Table 1 summarize the climate data for an average year in Djibouti.

TABLE 1: Djibouti climate table (Climatemps, 2018)

	Jan	Feb	Mar	Apr	May	Jun	Jul	Aug	Sept	Oct	Nov	Dec	Annual
Average Max Temperature °C	29	29	31	32	34	38	41	39	36	33	31	28	33.4
Average Min Temperature °C	23	24	25	26	28	30	31	29	29	27	25	23	26.7
Average precipitation mm	10	19	20	29	17	0	6	6	3	20	22	11	163.0
Number of wet days	3	2	2	1	1	0,5	1	1	1	1	2	2	17.5
Relative humidity %	69	71	73	74	70	53	43	44	60	65	67	71	63.3
Average dew point temperature (°C)	19	20	21.7	23.6	24.9	23.2	21.8	21.8	24.3	22	20.3	19.8	21.9

The average maximum temperature is in July, which is 41°C, and the average minimum temperature appears in December/January at 23°C. The number of the wet days is less than 20 days over the year as shown in the Figure 2.

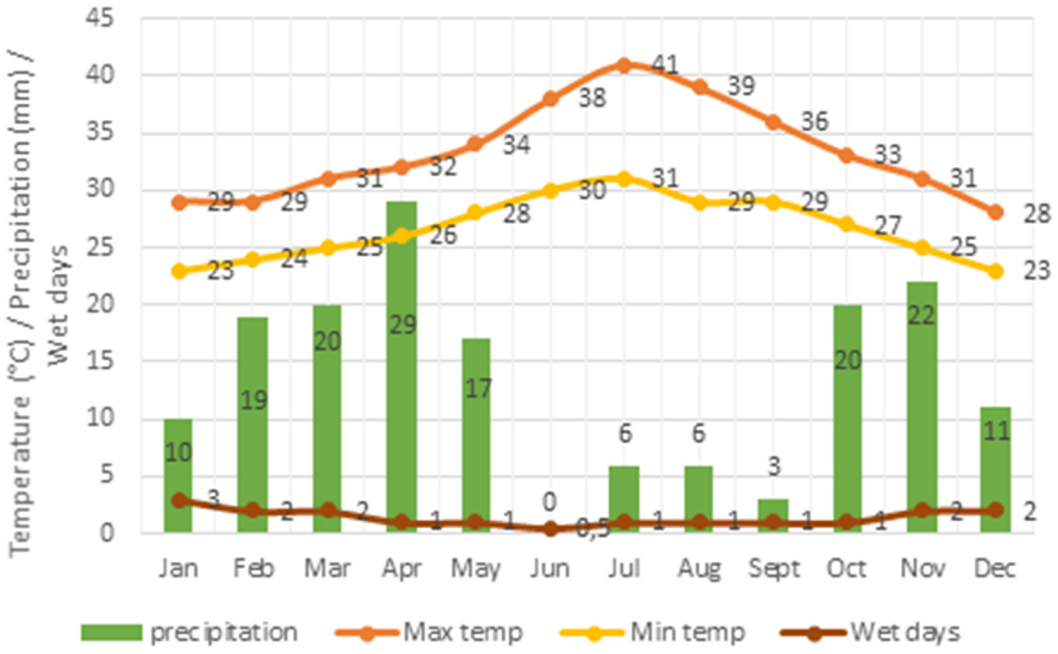

FIGURE 2: Djibouti climate graph

1.3 History of geothermal exploration

Geothermal exploration has a 47 years long history in Djibouti (in July 1967, the Colony of the French Somali Coast became the French Territory of the Afars and the Issas, and at independence on 27 June 1977 the Republic of Djibouti) and can be divided into six main historical phases:

The first geothermal exploration programme was launched in 1970 in Djibouti by BRGM (Bureau de Recherches Géologiques et Minières). BRGM is France's reference public institution for Earth Science applications in the management of surface and subsurface resources and risks.

a. The exploratory survey showed several possible potential geothermal areas and facilitated the quick identification of the Asal Rift as a target of major interest for geothermal exploration. In 1975, the first two wells were drilled, Asal 1 and 2 with a depth of 1146 and 1554 m respectively. They both showed good temperatures 260 and 235°C but only one of them has produced

geothermal fluid (Asal 1) but with a high mineralization fluid (120g/L). Well Asal 2 was damaged and well Asal 1 showed low production and was eventually plugged with sulphides scaling at the flash point in the well (BRGM, 1980).

In 1980, the second phase started and the Djibouti government has conducted a detailed general inventory of geothermal resources with the bilateral assistance of the Italian government (through Aquater Company) and the support of the World Bank (Aquater, 1981).

b. The Hanlé Plain was considered as a potential geothermal site, and an intensive exploration program was developed from 1981 to 1988 with the hope to find less saline fluids away from the salt-saturated site of Lake Asal. The exploration surveys led to the implementation of 3 geothermal gradient drillings at depths of 450 m as well as 2 deep exploration wells (at 1623 and 2038 m, respectively Well Hanlé 1 and well Hanlé 2). Two deep drillings in Hanlé met only low temperature aquifers, in well Hanlé 1, 72°C at 1420 m and in well Hanlé 2, 124°C at 2020 (Aquater, 1989).
c. Under the support of the World Bank, one of the condition was to stop financing the project if the third drilling fails. In this reason, the drilling was shift to the Asal area and therefore, the project continued with the drillings of Asal 3, Asal 4, Asal 5, and Asal 6 see Figure 3. Table 2 summarizes the wells drilled in Asal area characteristics.

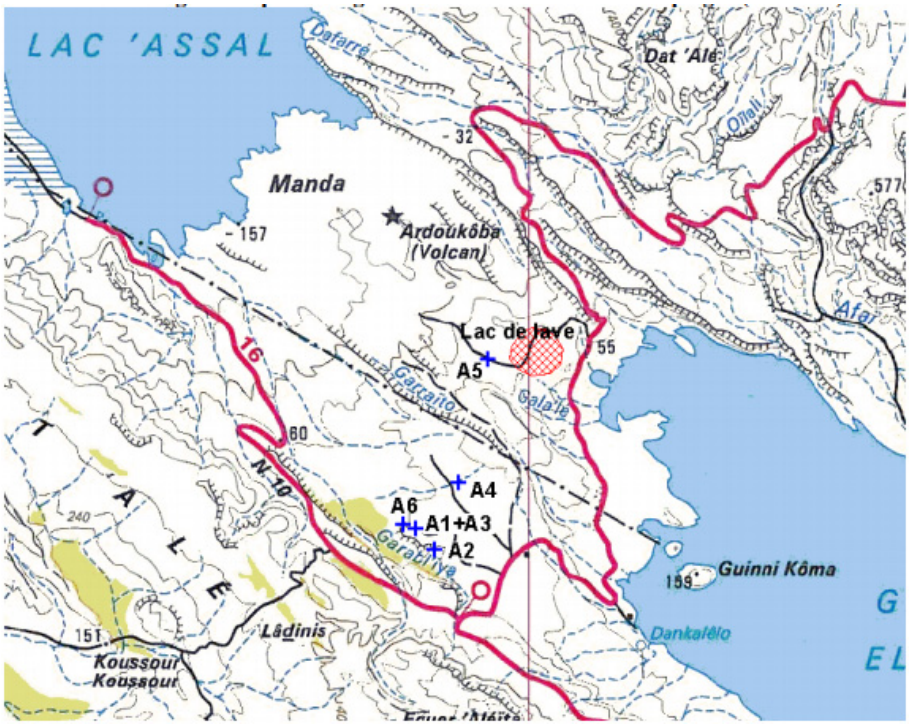

FIGURE 3: Geological map showing wells A1 to A6 (AfDB, 2013)

TABLE 2: Characteristics of Asal wells (Aquater, 1989; Souleiman, 2010)

Drilled Wells	Beginning of drilling	End of drilling	Final depth (m)	Temperature maximum (°C)	Total mass (ton/h)	Salinity (g/l)
Asal 3	11-06-1987	11-08-1987	1316	260	350 (WHP= 12.5 bar)	130
Asal 4	15-09-1987	20-12-1987	2013	345	-	-
Asal 5	7-01-1988	7-03-1988	2105	359	-	-
Asal 6	8-04-1988	10-06-1988	1761	280	150	130

d. The salinity of the deep reservoir fluid in the Asal geothermal field is high (120 g/L), about 3.5 times more saline than seawater. According to a preliminary study of A3, and the analysis of scaling deposits in A6, as reported by Aquater (1989) in its final report, the fluid discharge from these wells resulted in such a large amount of solid deposits as to seriously compromise well production.

From October 1989 to April 1990, the third phase started:

e. Scaling and corrosion study has been carried out by Virkir Orkint, Icelandic company. Second production test has been performed by flowing Asal3 well. Wellbore scaling of Asal3 well has been studied and some scale inhibition chemicals have been used in attempt to alleviate the scaling problem. But the program again failed on commercial developments due to these difficult fluid conditions (Virkir-Orkint, 1990).

The fourth phase started more recently (from October 2007 to March 2008):

f. The Icelandic company named Reykjavik Energy Invest (REI) performed a new prefeasibility study in the Asal rift zone. The results of this study were found conclusive and REI offered to proceed to the next feasibility and development phases. Due to the financial crisis in Iceland, REI did not succeed to perform the feasibility study planned initially; this situation placed the project in standby and it was abandoned afterwards.

The fifth phase was launched in 2011 by the government of Djibouti with the support of a financial consortium led by the World Bank with AFPB, OPEC fund and eventually GEF and AFD engaged a new proposal in the Asal area. The total funding for this project is estimated around 31 MUSD

g. This project is presently on going and four wells have been planned to be drilled down to 2800 m with large production diameters (9 inches) and deviated in the reservoir (below 2000 m) in order to maximize the chances to intersect open productive fissures supposedly vertical in this axial part of the rift (AfDB, 2013).

The sixth phase coincides with the creation of a new organization exclusively dedicated for geothermal development in Djibouti named ODDEG (Djibouti Office for Geothermal Energy Development) in 2014. Several bilateral and multilateral projects were launched:

1) With the assistance of Japan International Cooperation Agency (JICA), ODDEG carried out in 2014 a data collection survey to summarize and analyse all geological and geochemical information on thirteen geothermal sites in order to prioritize the development of the country (JICA, 2014). The Hanlé-Garabayyis was considered as a first potential geothermal site. An intensive exploration program was undertaken, and Djiboutian and Japanese expert conducted geological, geochemical and geophysical together with socio-environmental surveys. The exploration surveys concluded to the implementation of 3 geothermal drillings at depths of 1500-2000 m in 2018.

2) Partnership Agreement between The Government of Djibouti and ICEIDA (Icelandic International Development Agency) for the Geothermal Exploration Project was established from 2013 in order to build capacity within the recently established (ODDEG) in geothermal drilling and exploration as well as assist with institutional development of the ODDEG through training in geothermal projects management.
   - Under this assistance, geothermal surface exploration was carried out in the Lake Abhé prospect, Djibouti in November and December 2015 by ÍSOR and ODDEG. The project was financed by (ICEIDA) and the Nordic Development Fund (NDF).

3) The Arta geothermal prospect is one of the several geothermal prospects in Djibouti, and on the southern shore of Tadjourah gulf. This site was submitted to the GRMF (Geothermal Risk Mitigation Facility) third round for a surface study program and in 2015, this site was selected to receive the grant after application submission. The plan survey will be including, geology,

geochemistry, geophysics including environmental and social survey. Now this site is on preparation for finalizing process with the GRMF committee to sign the grant agreement. Active work will start later on November after grant signing.

1.4 Geothermal regulatory framework

Concerning the institutional aspects, the government of Djibouti has taken several initiatives to develop and promote its geothermal resource. Figure 4 depicts the organizations related to energy policies in Djibouti.

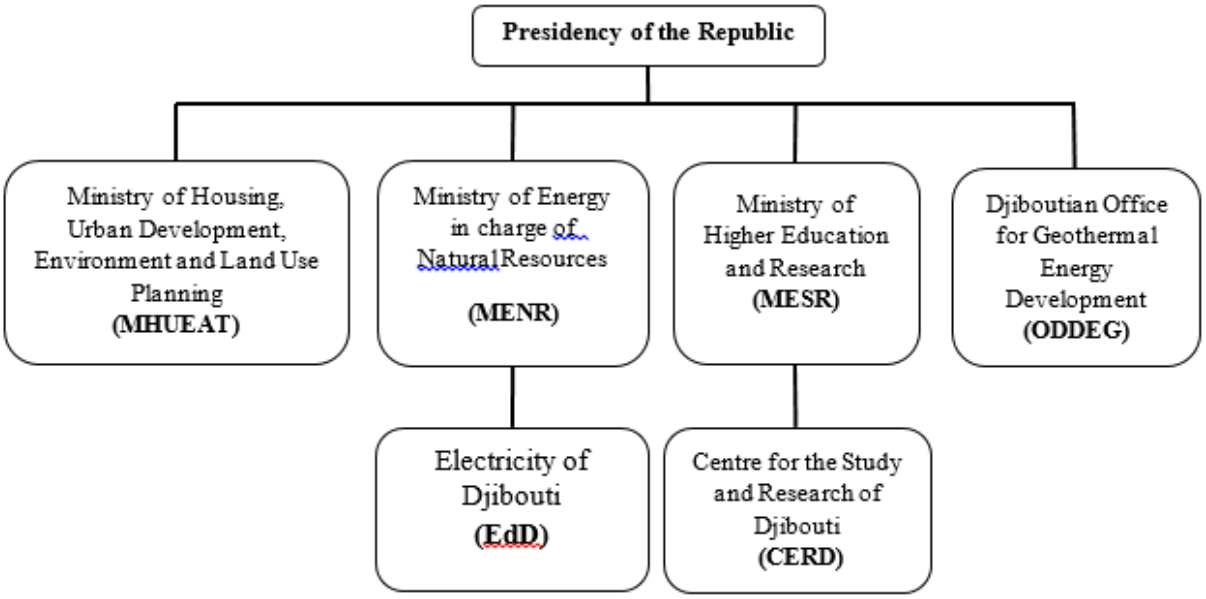

FIGURE 4: Energy sector organization in Djibouti

According to the decree N°2016-148/PRE establishing the responsibilities and duties of the ministries, the Ministry of Energy in charge of Natural Resources is responsible for the development and implementation of sectoral policies in the fields of energy and natural resources, promotion and development of the exploitation of resources mining and oil and renewable energy sectors. As such, it prepares and executes the government's energy policy, notably through a policy of investment and development of alternative energy sources. The Electricity of Djibouti (EDD) is under the supervision of the Ministry.

- Electricity of Djibouti is the power utility company in charge of generation, transmission, distribution and selling energy in Djibouti.
- Law No.88/AN/15/7th regulating the activities of independent electricity producers enters into force on 01 July 2015. This law of liberalization of energy production aims to:
    - Promote private sector participation and competition in the production of electric power;
    - Define the legal framework to develop the production of electric power by private operators.
    - According to the Law No.138/AN/16/7th L of July 23rd, 2016 of the Mining Code, concessions and permits are issued by the Ministry of Energy.

Ministry of Housing, Urban Development, Environment and Land Use Planning is in charge of the government's policy on the environment, in particular, the drafting of normative texts, the monitoring of environmental standards in the fields of infrastructure, housing, equipment, transport, energy in partnership with relevant ministries and carrying out environmental impact assessments (EIA). There are two decrees concerning for EIA in Djibouti:

- Decree No. 2001-0011/PR/MHUE is concerning definition of the environmental impact assessment procedure and the environmental management of major projects.
- Decree No. 2011-029/PR/MHUE revises the environmental impact assessment procedure.

A full EIA should be carried out prior to the drilling and plant construction should include Environmental Management Plans and costs in the project's design and budget. The environmental permit is issued by the ministry of environment for a period of five years from the start of the project and is renewable after an environmental audit.

The ministry of higher education and research is responsible for overall research studies. ISERST, which is formerly CERD, was established on January 1, 1979 for the purpose of investigating natural resources. It was reorganized and became Centre for Study and Research of Djibouti (CERD) in 2001, the CERD is in the main institution for scientifically research. It has a well-equipped geochemistry laboratory.

ODDEG, the only institution exclusively dedicated for geothermal in Djibouti was created in 2014. The geothermal energy is a key sector for the economic and social development of the country. With the strong commitment of the Government, geothermal development was putted in a high-level priority. In this reason, it was placed under the direct umbrella of the presidency. ODDEG is empowered to undertake all activities related to the geothermal resource development in order to make available geothermal resource for IPPs. The main duties of ODDEG are:

- Identification of the various types of geothermal resources of the country
- The completion of exploration, reconnaissance and research work
- Conducting pre-feasibility studies and feasibility studies for the industrial development of these resources and the diversification of their uses.

1.5 Objective of the study

The objective here is to determine how the medium-enthalpy resource in Lake Abhe geothermal field would be best utilized, both technically and commercially. The backbone of this paper will be how to deal with the hot, arid climate in order to maximize the net power output of the plant. Resource assessments will be performed in order to provide the information about reservoir data such as; total flow rate, reservoir temperature and pressure, and the expected total power generation. Binary power plant is planned to be placed at the located area. The geothermal power plant will work on ORC (Organic Rankine Cycle). A thermodynamic model will be developed using Engineering Equation Solver (EES) to evaluate the performance of ORC geothermal power plants standalone with different cooling system, and an ORC assisted by a parabolic trough solar concentrating collector field. The selection of the working fluid will be evaluated; the suitable working fluids should be taken in the consideration on the system performance analysis with a screening criteria based on the maximum net power output, thermal efficiency and specific power output SPO. Finally, economic analysis will be performed in order to assess the cost of developing the binary power plant in Lake Abhe geothermal field according of the best two scenarios.

2. RESOURCE ASSESSMENT

2.1 Geology

The location of the Republic of Djibouti is unique in terms of geodynamics activity. It is situated at the eastern extreme of the Afar depression. The Afar depression is one of the unique geological settings on the Earth today see Figure 5. It represents the only modern example of continental rifting at an active triple-junction, where two oceanic ridges, Gulf of Aden and Red Sea, meet with East African Rift (Tazieff et al., 1972).

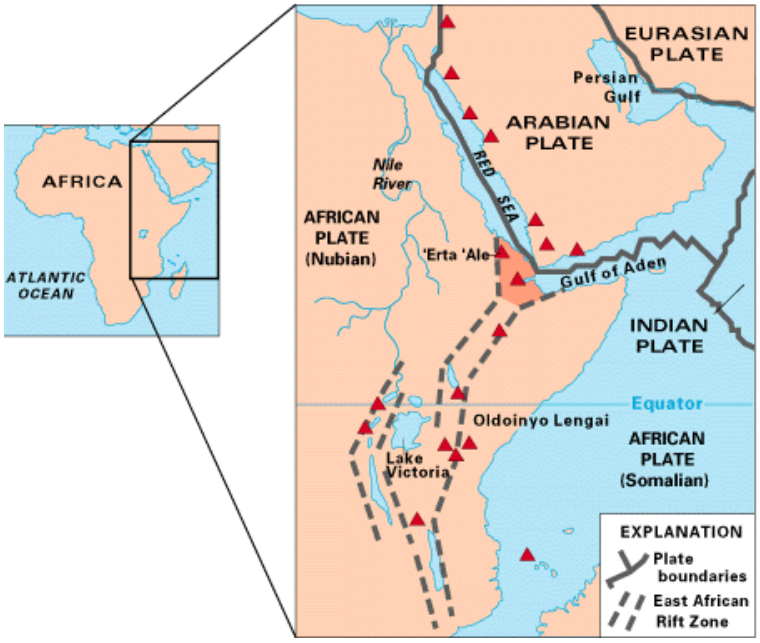

FIGURE 5: Location map of the Afar Triangle (the shaded area in the centre of the map) and the East African Rift zones; red triangles show historically active volcanoes (Smithsonian Institution, 2018)

The Gulf of Aden and the Red Sea, spreading created these young, narrow seas and active rifting continues to widen them into new ocean basins. The third arm of the triple junction is the East African Rift system, which runs North-South and was formed by the separation of the African and Arabian tectonic plates beginning over 35 million years ago. The East African Rift Valley may represent a failing rift that will not develop into a new ocean basin; the African rift is spreading at a rate of only 6mm/year in contrast to the 2 cm/year divergence along the other two rift arms (Bagley et al., 2004).

With regard to the geological formations that are in the Djibouti Republic, it is found that the volcanic rocks dominate the Djiboutian territory. Almost all the rock composition in the country is basaltic as shown in Figure 6, it is composed by the Dalha basalts (8-4 My), Somali basalts (5-3 My), Stratoid basalts (3.5-1 My). Quaternary sedimentary rocks are the most recent formations and are distributed over coastal areas and large basins within the land (Hanlé Basin, Gobaad and Gaggade) shown in yellow in the Figure 6.

Located in the southeast part of the Afar depression, the Republic of Djibouti has been the place of an important tectonic activity since the Oligo-Miocene period until today. Hence, a huge quantity of energy is dissipated from the very shallow earth mantle to the surface, and the Afar triangle is the only region in the world along with Iceland where an oceanic ridge is accessible off shore for geothermal exploitation. Figure 6 depicts in dots, the surface manifestation located mainly on the rift stream bed (SW-NE trend) where the red dots and the blue dots represent the numerous hot springs and the fumaroles respectively.

2.2 Geological features of Lake Abhé

Lac Abhé is located on the border between Ethiopia and Djibouti. One part is in Ethiopia and the other part is in Djibouti. This lake takes its name from the local language and Abhe means rotten describing the fumarolic smell emitted by the chimneys.

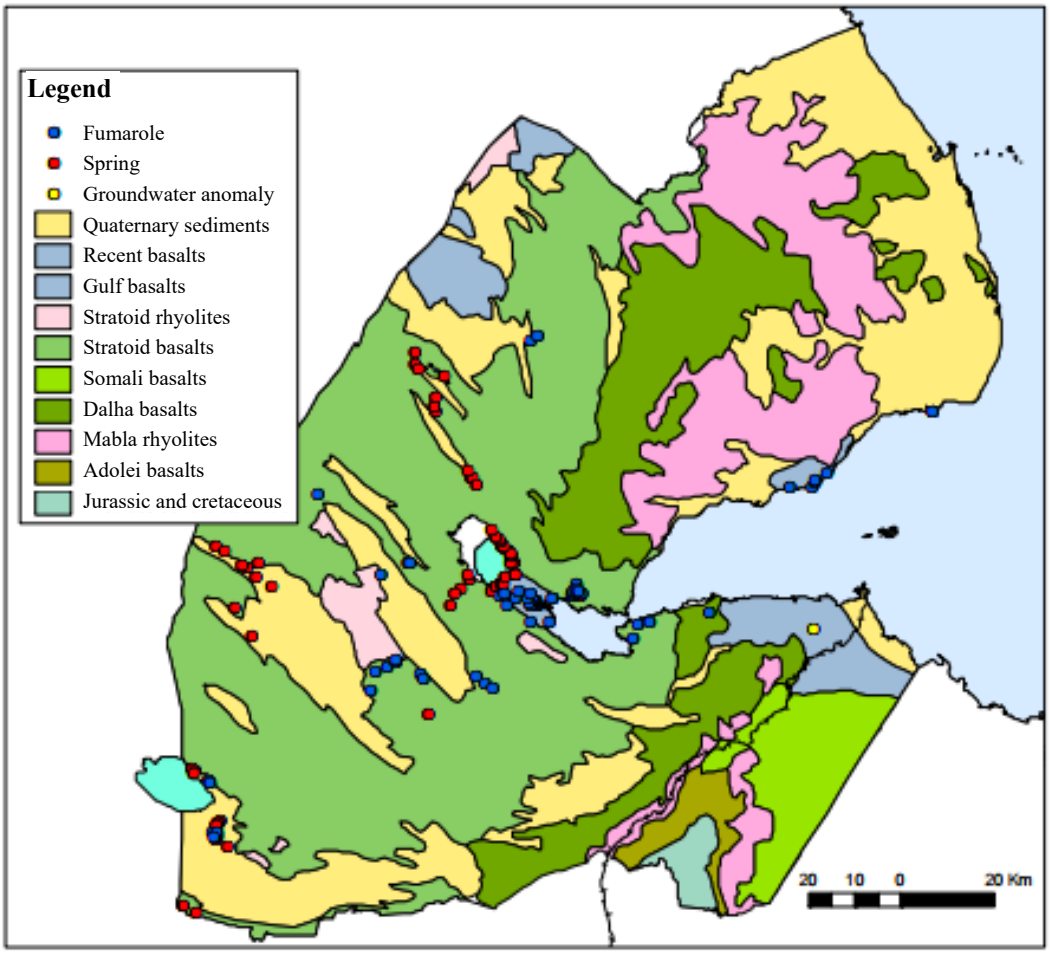

FIGURE 6: Geology and hydrothermal manifestations (Jalludin, 2012)

This closed lake has its source from Ethiopia where it is fed by the river Awash. It has the peculiarity of being an endorheic lake, i.e. that the lake normally retains water and allows no outflow to other external bodies of water, such as rivers, seas or oceans and that the evaporation is the only way for it to be lost.

The open water area of the lake is close to 34 000 ha with a maximum depth of 37 m and an average of 8.6 m depth. However, in recent years successive droughts and the extraction of the water for irrigation has greatly reduced this area. The Lake surface had shrunk to two thirds of what it was in the late 1940s. This shrinkage is evidenced by extensive saltflats now covering some 11 500 ha to the southwest of the Lake. A small part of these flats extends into Djibouti see Figure 7.

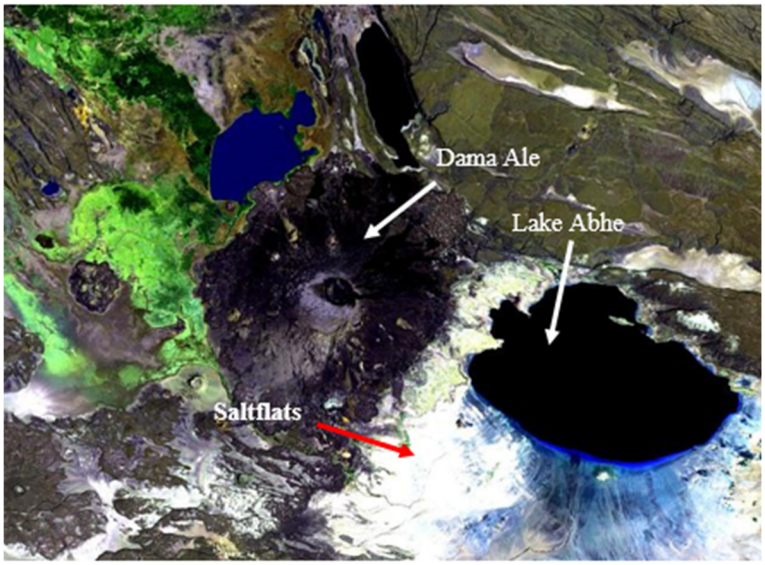

FIGURE 7: Satellite image of Dama Ale volcano (in the middle) and the Lake Abhe (to the right) (Global Volcanism Program, 2018)

The volcanic peak of Dama Alé (1069 m) dominates the northwestern shoreline of the lake as showing in the Figure 7, while vast saltflats, locally 10 km wide, extend around the southwestern and southern shores (Hughes and Hughes, 1992).

2.2.1 Travertine

At sunset, Lake Abhe offers an extraordinary spectacle where all the tourists of the world covet this unique lunar landscape to immortalize this moment. These unique features attracted the director of the saga "planets of apes" from where the first film was shot in 1968 at Lake Abhe. As far as the eyes can see, there are quite a lot high chimneys of travertine; the highest one reaches 60 meters high and has a diameter of about 90 m. The peak of these chimneys of travertines escapes the smoke of fumaroles. Moreover, to their foots flow most of the hot springs as depicted in Figures 8 and 9.

FIGURE 8: Hot spring in Lake Abbe (Cosar, 2018)

FIGURE 9: Fumaroles at the top of limestone chimneys (Travel Adventures, 2018)

These travertines were formed several thousands of years before the Lake lose a significant water and they were immerged. These result from the mixing of Ca-rich spring waters with saline, carbonate-rich lake water leading to immediate precipitation of calcium carbonate (Pentecost and Viles, 1994). The growth rate of modern travertines reaches a few centimetres per year. The growth of travertines is governed by chemistry of parental solution and the rate of CO_2 degassing, which decide upon effective precipitation of calcium carbonates (Gradzinskiet al., 2015).

Geologically, the lake Abhe area is mainly composed of stratoïd basalts with a high plateaus limited by E-W faults configuring the Gobaad plain. Several rhyolitic intrusions-pyroclastic are distributed along the southeastern margin. The area is still in formation due to the ongoing movement of the divergent plate boundary. The travertines are aligned on the main fracture trends. Major WNW fracture systems are parallel to graben and horst structures, while minor transversal NNE trend fractures are also recognized. Surface hydrothermal manifestations are numerous around the lake, a fumarole and rich variety hot springs and many travertine constructions. Geochemical data show that the lake does not recharge the geothermal reservoir. Based on the geochemical- and geological data, the reservoir is mainly thought to be recharged from higher altitudes WNW of the geothermal field (Figure 10). Recharge may also occur along the WNW-ESE graben faults east of the lake

2.3 Geochemistry

Geochemical study of thermal water from Abhe Lake area is carried out from 1975 to 2014 in order to investigate the origin and sources of solutes and estimate the subsurface reservoir temperature.

The first geochemistry study done in 1980 by Aquater classified the water from Lake Abhe in two groups. Most of the hot springs are alkaline-chloride-sulphated and few of them present a bicarbonated type as a result of surface water mixing. And the geothermometer indicated a temperature in the range of 137-176°C (Aquater, 1981).

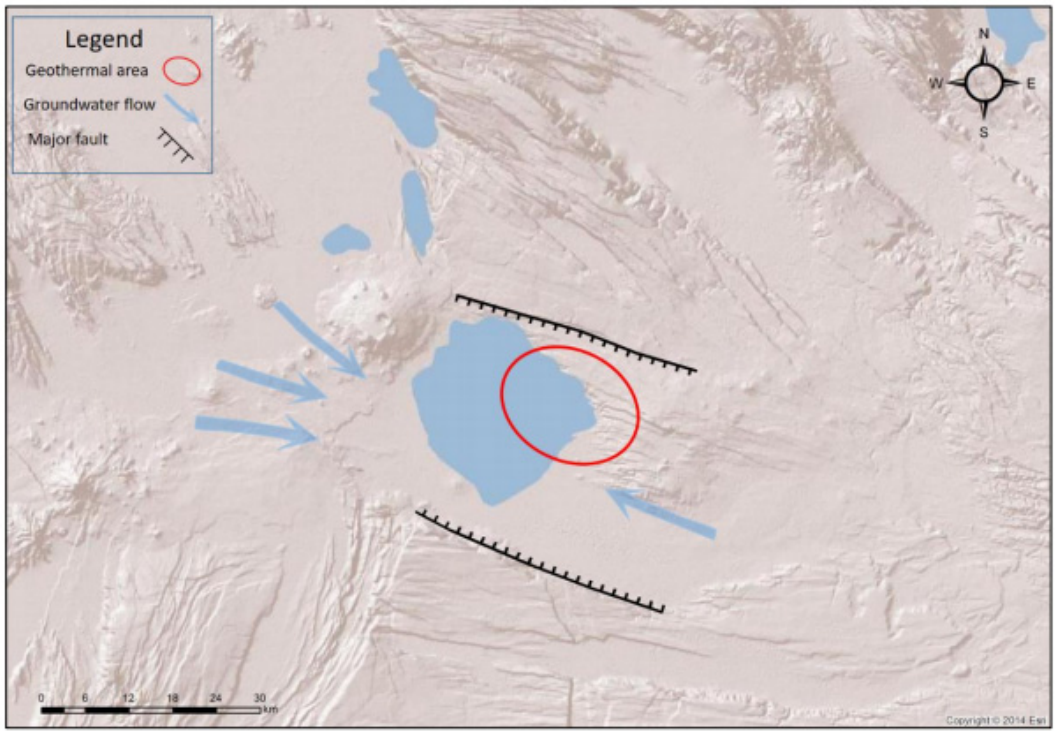

FIGURE 10: Estimated recharge of the geothermal system and the main faults orientation (ODDEG-ISOR, 2016)

The CERD undertaken in 2009 surface exploration in Lake Abhe area. The geochemical team with its leader Dr. Houssein collected 21 water samples from cold and hot springs. They concluded that the hot springs from the Lake Abhe area are characterized by Na-Ca-Cl type of water with a temperature of the hot spring varies from 88,8 to 99,7°C. The total dissolved solids of this group range from 1700 to 3400 mg/l (Bouh, 2010). The result of the geothermometer shows that the reservoir temperature can be reach up to 150 ºC (Bouh, 2010).

In 2014, the CERD redid another geochemical survey. Chemical (mainly Na/K and SiO_2), isotope (bisulfate- and anhydrite- water), and multiple mineral equilibrium approaches were applied to estimate the reservoir temperature of the hot springs in the Lake Abhe geothermal field. These different geothermometric approaches estimated a temperature range of the deep geothermal reservoir of 120–160°C. In spite of the relatively wide range, the three different approaches led to a same mean of about 135°C. (Awaleh et al., 2015).

Recently the study done by ODDEG and ISOR jointly indicate a low enthalpy geothermal system with reservoir within a range of 110–150° C. The estimated total water flow from the manifestations is around 20-25 L/s (ODDEG-ISOR, 2016).

Geochemical data show that the lake does not recharge the geothermal reservoir. Based on the geochemical- and geological data, the reservoir is mainly thought to be recharged from higher altitudes WNW of the geothermal field (Figure 7). Recharge may also occur along the WNW-ESE graben faults east of the lake. There are two types of geothermal springs in LAGF:

- Those jetting around the base of the Great Travertine Chimneys (GHCi samples);
- Those occurring at the bottom of Small Travertine Chimneys (SHCi samples).

Temperature, pH, electrical conductivity (EC), total dissolved solids (TDS), sampling locations, and hydrochemical types of all water samples are listed in Table 3. This table is modified from (Awaleh et al., 2015). The temperatures of the geothermal water samples at Lake Abhe geothermal field ranged

from 71 to 99.7°C (Table 3). Geothermal waters are moderately alkaline (pH = 7.61–8.79) with TDS values of 1918–3795 mg/L. The geothermal waters contain Cl^- and Na^+ as the predominant anion and cation. The chemical composition of the waters is described in terms of relative concentrations of the main anion and cation, which allows discrimination of the following two groups of waters. Geothermal hot spring waters are of the Na–Cl type. Lake Abhe waters are of the Na–Cl–HCO_3–SO_4 type.

TABLE 3: Sampling locations, T, pH, EC, TDS and hydro-chemical types of the sampled waters (Awaleh et al., 2015)

N°	Samples		Latitude 00°00′00″	Longitude 00°00′00″	T °C	pH	EC (μS/cm)	TDS (mg/l)	hydrochemical types
1	**SHC1**		11°08′53.2″	041°52′51.9″	94.5	8.22	5495	3488	Na – Cl
2	**SHC2**		11°08′41.4″	041°52′54.1″	98.1	8.34	5576	3482	Na – Cl
3	**SHC3**		11°08′50.9″	041°52′52.8″	98.5	8.49	5610	3503	Na – Cl
4	**SHC4**		11°08′53.0″	041°52′50.2″	82.2	7.61	5866	3747	Na – Cl
5	**SHC5**	**Geothermal**	11°08′54.7″	041°52′44.9″	98.8	8.33	5332	3466	Na – Cl
6	**SHC6**	**spring**	11°08′54.7″	041°52′44.7″	98.1	7.97	5409	3795	Na – Cl
7	**SHC7**	**waters**	11°08′54.6″	041°52′44.4″	97.1	8.06	5411	3511	Na – Cl
8	**GHC1**		11°06′49.6″	041°52′30.1″	92.1	8.6	3224	2129	Na – Cl
9	**GHC2**		11°06′49.8″	041°52′13.2″	71	8.62	3191	1958	Na – Cl
10	**GHC3**		11°06′46.5″	041°52′12.7″	86	8.52	3192	2236	Na – Cl
11	**GHC4**		11°06′46.7″	041°52′11.9″	99.7	8.69	3124	2072	Na – Cl
12	**GHC5**		11°06′47.1″	041°52′10.6″	84.2	8.72	3138	2023	Na – Cl
13	**GHC6**		11°06′48.6″	041°52′09.5″	92.5	8.62	3105	2016	Na – Cl
14	**GHC7**		11°06′48.6″	041°52′09.6″	82.4	8.79	3124	1918	Na – Cl
15	**GHC8**		11°06′49.6″	041°52′10.0″	93	8.69	3095	2037	Na – Cl
16	**GHC9**		11°06′50.6″	041°52′39.0″	76.6	8.11	3314	2089	Na – Cl
17	**Lake Abhe**	**Lake water**	11°09′52.2″	041°53′24.2″	29	9.86	96084	92622	Na – Cl – HCO_3 – SO_4

2.4 2D model and drilling target

A resistivity survey was carried out in 2011 by the CERD and 2015 by ODDEG-ISOR in the Lake Abhé prospect with a total of 84 MT soundings and 53 TEM soundings. Data from 53 TEM and MT sounding pairs have been 1D jointly inverted. A total of 66 stations was measured at the same time in 2015 by ODDEG team.

The resistivity model shows a low resistivity layer (resistivity less than 5 Ωm) reaching to the surface. It is about 300–400 m thick in the western part of the survey area and becomes thinner to the east, show in the Figure 7 by the yellow area (ODDEG-ISOR, 2016).

Below this layer at the centre of the survey area, another low resistivity layer is revealed (resistivity less than 10 Ωm) and is depicted in turquoise colour on Figure 11. It coincides with the geothermal surface manifestations and is presumably connected to geothermal fluid and/or geothermal alteration. This conductive structure can correspond to the permeable stratoid basalts outcropping in the eastern part of the area (ODDEG-ISOR, 2016).

The resistive formation below the low resistivity can be associated with the less permeable stratoid basalts or a rhyolitic formation. At greater depths (more than 2,500 m) a deep-lying low resistivity is seen in the western part of the area, presumably associated with Pleistocene sedimentary formations. This sedimentary unit probably corresponds the oldest rocks in Djibouti, which are observed in the southern part of Djibouti (Ali-Sabieh region) (ODDEG-ISOR, 2016).

The geothermal system in Lake Abhe is presumably fracture dominated with near vertical conductive fractures. Based on results from various geoscientific disciplines, it can be concluded that the hydrothermal fluids flow from the Ethiopian side (below the lake). The existence of the volcano Dama Ale and presence of the surfaces activities at the other side of the lake are consistent with ODDEG-ISOR hypothesis, and a possible magma body below the volcano may act as the heat source for the surface activity east of Lake Abhé (ODDEG-ISOR, 2016).

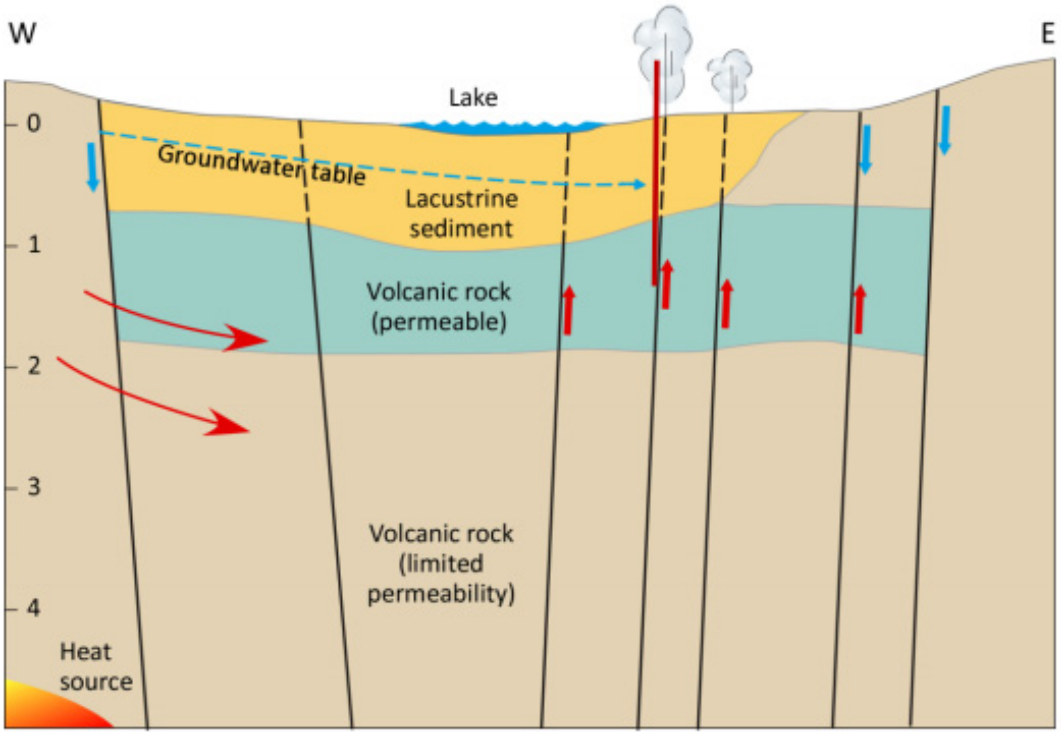

FIGURE 11: Geological cross-section; a well drilled to more than 1000 m depth, intersecting one of the main permeable fault in the system is shown as a red vertical line on the cross-section (ODDEG-ISOR, 2016)

The geothermal liquid emerging to the surface on the Djiboutian side may also be due to deep circulation of water into rocks with abnormally high thermal gradient. The high thermal gradient may either be due to proximity with the Dama Ale volcano or due to crustal thinning (ODDEG-ISOR, 2016).

The conductive zones go from 900 m up to 1500 meters before showing higher resistivity. The major normal faults in the area are also thought to facilitate fair permeability. Based on this, future wells should be drilled to more than 1.000 m depth and targeting one of the major faults in the area (Khaireh et al., 2016).

2.5 Volumetric assessment

The volumetric method refers to the calculation of thermal energy in the rock and the fluid, which could be extracted, based on specified reservoir volume, reservoir temperature and reference or final temperature.

The volumetric method is patterned from the work applied by the USGS (United States Geological Survey) to the Assessment of Geothermal Resources of the United States (Muffler, 1979). It is often used for first stage assessment, when data are limited. The main drawback of this method is that the dynamic response of a reservoir to production is not considered, such as pressure response, permeability, recharge, etc.

2.5.1 Thermal energy calculation

For a liquid-dominated reservoir, the equations used for calculating the thermal energy are as follows:

$$Q_t = Q_r + Q_w \quad (1)$$

in which

$$Q_r = A.h.(1-\emptyset).\beta_r.\rho_r.(T-T_r) \quad (2)$$

$$Q_w = A.h.\emptyset.\beta_w.\rho_w.(T-T_r) \quad (3)$$

where Q_T = Total thermal energy (kJ/kg);
Q_r = Heat in rock (kJ/kg);
Q_w = Heat in water (kJ/kg);
A = Area of the reservoir (m^2);
h = Average thickness of the reservoir (m);
$\emptyset$ = Rock porosity;
β_r = Specific heat of rock at reservoir (kJ/(kg°C));
β_w = Specific heat of water (kJ/(kg°C));
ρ_r = Rock density (kg/m^3);
ρ_w = Water density (kg/m^3);
T = Average temperature of the reservoir (°C);
Tr = Reference temperature (°C).

Not all the energy can be extracted from the reservoir, so the recovery factor is defined to help estimate the energy that can be extracted. The thermal energy recoverable from the system can be calculated as follows:

$$Q_R = R.Q_r \quad (4)$$

where Q_R = Recoverable thermal energy (kJ/kg);
R = Recovery factor.

The recovery factor represents how easily the heat contained in the reservoir can be extracted which mostly depends on the reservoir permeability. Muffler proposed a linear connection between the porosity and the recovery. (Muffler, 1979) and (Williams, 2007) introduced models for fractured reservoir and proposed recovery in the range of 2-25%.

The parameters used in the Monte Carlo volumetric assessment calculation for the Lake Abhe reservoir are presented as follow.

Area (km^2): The surface area of the geothermal system is estimated by three mains different methods.

- The surface manifestation that usually gives the minimum area.
- The resistivity measurement is another method to estimate the surface area of a geothermal system, it is the most accurate method and MT (MT is a geophysical method that measures naturally occurring, time-varying magnetic and electric fields) is mostly used because we can measure the resistivity of the subsurface from the very near surface to 10 km.
- The thermal gradients measured in shallow wells. It is a physical quantity that describes in which direction and at what rate the temperature changes the most rapidly around a particular location. It is expressed by in units of degrees Celsius per unit length (°C/m). It is less accurate than the resistivity measurements because a shallow geothermal system can induce the measure in error.

In our case the surface was estimated by the MT method and the total area of lake Abhe's surface geothermal area is estimated at 75 km^2 (Appendix I). For Monte Carlo calculations, the most likely area is: 75 km^2; minimum: 70 km^2; maximum: 88 km^2.

Thickness (m): The thickness of the permeable volcanic rock formation ranges from 500 to 1500 m. This thickness is characterized by the turquoise colour area shown in the Figure 11. For Monte Carlo calculations, use the most likely: 1000 m; minimum: 800 m; maximum: 1200 m.

Rock density (kg/m^3): The system is composed mainly of basalt volcanic rock, which have a density of around 2900 kg/m^3 (Stacey and Davis, 2008). Therefore, the most likely estimate is 2900 kg/m^3; minimum: 2600 kg/m^3; maximum: 3100 kg/m^3.

Porosity (%): The average porosity in the basalt rock in Djibouti is given by (Shao-Qianq, 2015) and it is 10%. In the Monte Carlo input cell, use the most likely: 10%; minimum: 5%; maximum: 20%.

Rock specific heat (J/(kg°C)): Usually this is about 950 J/(kg°C). For the Monte Carlo calculations is fixed at 950 J/(kg°C).

Reservoir temperature (°C): The different geochemistry study since 1981 indicated a geothermometer temperature in the range of 110-176°C. For the Monte Carlo calculations, it is assumed that the most likely value is 150°C; minimum: 110°C; maximum: 176°C.

Fluid density (kg/m^3): Water density is 950 (most likely), 917 (minimum) and 891 kg/m^3 (maximum) at 110, 150 and 176°C, respectively.

Fluid specific heat (J/(kg°C)): It is about 4200 J/(kg°C) for pure water.

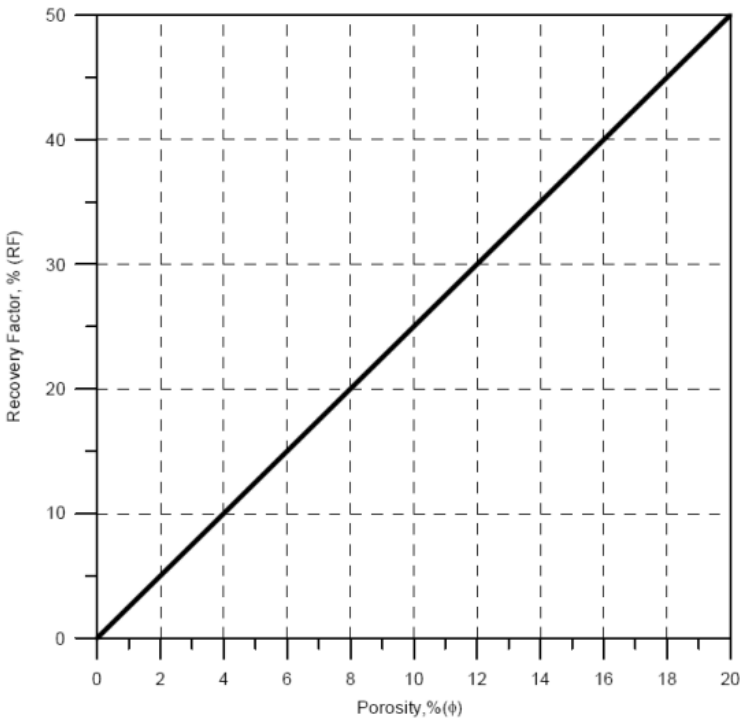

FIGURE 12: Correlation between recovery factor and porosity (Sarmiento and Steingrímsson, 2011)

Recovery factor (%): Recovery factor refers to the fraction of the stored heat in the reservoir that could be extracted to the surface. Muffler proposed a linear correlation between porosity and recovery factor. Figure 12 shows the theoretical geothermal recovery factor as a function of the reservoir porosity (Sarmiento and Steingrímsson, 2011) and (Muffler, 1979). The porosity basaltic reservoir ranges from 5 to 20% with the average of 10%.

The estimated most likely recovery factor of Lake Abhe reservoir is 25%, the minimum 20%, and the maximum value will be 30%.

Reference temperature (°C): The reference temperature is the temperature of the state from which the heat is integrated

- The ambient temperature;
- The abandonment temperature;
- The minimum temperature for space heating.

Most of the time, it is similar to the abandonment temperature or at ambient temperature. The choice of the reference temperature depends on how one calculates the usable energy. Here the average abandonment temperature of 90°C is taken as the reference temperature.

2.5.2 Power plant sizing

The equation that applies for converting the heat reserve into electrical power is given as:

$$P = \frac{(Q_t \,.\, R_f \,.\, C_e)}{P_f . t} \tag{5}$$

where P = Power potential (MWe);
R_f = Recovery factor;
C_e = Conversion efficiency;
P_f = Plant capacity factor; and
t = Time in years (economic life):

Power plant factor (%): The availability factor of a power plant is the amount of time that it is able to produce electricity over a certain period, divided by the amount of the time in the period (*Plant factor = Operating days / Calendar days*). The good performance of many geothermal plants around the world places the availability factor to be from 90-97 %. In our case, the plant factor is fixed at 95%.

Power plant life cycle (years): The economic life of the project is the period it takes the whole investment to be recovered within its target internal rate of return. This is usually 25-30 years. In our case, it is set at 30 years as economic life.

Conversion efficiency: The conversion efficiency takes into account the conversion of the recoverable thermal energy into electricity. In their paper Garg and Combs (Garg and Combs, 2011), summarized that the second law of efficiencies conversion ranges between 25 and 45% in a resource assessment of several low temperatures geothermal fields in most operating ORC plant. In our case, the estimated most likely conversion is 40%, the minimum 35%, and the maximum value will be 45%.

2.5.3 The input cells

The uncertainty of reservoir parameters requires that they be estimated. For this reason, a Monte Carlo simulation is carried out. The Monte Carlo Simulation program is embedded in MS Excel spreadsheet. This spreadsheet for volumetric reserves estimation belongs to the Reykjavik University.

The simulation allows the inputs parameters to vary from a range of possible minimum to maximum values. Rock specific heat, average reservoir depth, rejection temperature, plant capacity factor and project lifetime have been only fixed. The values within the range are calculated at random according to a *Beta* or *Even probability distribution function*. To obtain a good representation of the distribution sampling is done through 2000 iterations with continuous calculation.

TABLE 4: Volumetric assessment parameters and their probability distribution for Lake Abhe

Parameter	Unit	Minimum	Most likely	Maximum	Distribution
Reservoir area (A)	km^2	70.0	75.0	88.0	Beta
Reservoir thickness (H)	m	800	1000	1200	Beta
Reservoir temperature (T)	°C	110	150	176	Beta
Recovery factor (R)	%	5%	10%	20%	Beta
Utilization factor (u)	%	35%	40%	45%	Beta
Porosity (fi)	%	5%		20%	Even
Specific heat of rock (CR)	$kJ/m^3/°C$		950		Fixed
Average reservoir depth (D)	m		1500		Fixed
Rejection temperature (Ta)	°C		90		Fixed
Plant capacity factor (F)	%		95%		Fixed
Project lifetime	years		30		Fixed

2.5.4 Results

The distributed frequency and the potential electrical power for Lake Abhe are shown in Figure 13. The results of the simulation show that the Lake Abhe reservoir has a most likely potential between 12.8 and 16.1 MWe for 30 years.

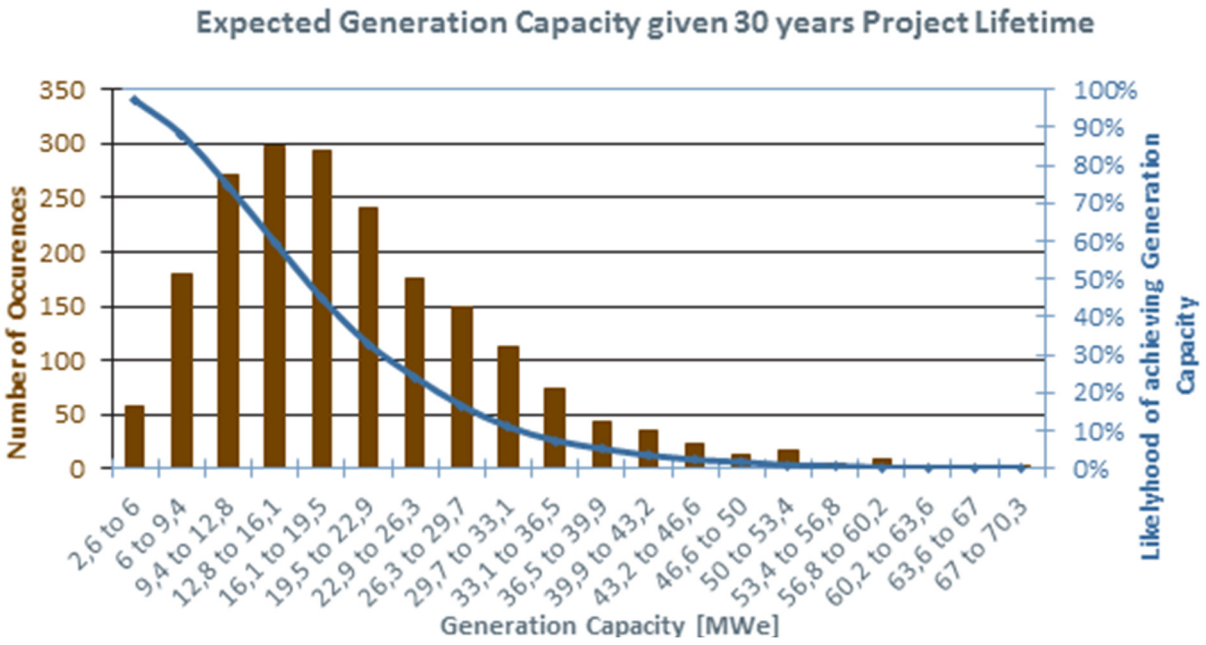

FIGURE 13: Frequency and cumulative frequency distributions for the reserve estimate of the Lake Abhe geothermal field

TABLE 5: The results of the thermal power estimation for the Lake Abhe reservoir by the Monte Carlo volumetric assessment

Capacity (MW)		
90%	Most Probable	10%
8.8	**14.45**	33.9

The results of the simulation show that the Lake Abhe reservoir has potential between 12.8 and 16.1 MW_e for 30 years. The cumulative frequency distribution indicates that the most likely value for the reserve is 14.45 MW_e. The cumulative frequency graph also illustrates that there is less than a 10% chance that the reserve will be above 33.9 MW_e. On the other hand, there is a 90% chance that the reserve will yield 9 MW_e.

According to Monte Carlo volumetric resource assessment, the most probable range of generation is between 12.8 to 16.1 MWe. The total energy output of the power plant will the most likely power set after calculation by the previous method at 14.45 MW_e.

Theoretically, the maximum amount of energy that can be extracted from the reservoir is given by the energy balance equation, (Çengel and Boles, 2015):

$$W = \dot{m} C_P (T_{Geo} - T_{Ret}) \eta \quad (6)$$

where $\dot{m}$ is the geothermal brine mass flow from the reservoir, C_P is the specific heat capacity of water, T_{Geo} is the temperature of the resource at extraction, and T_{Ret} is the rejection temperature and η is thermal efficiency of binary unit (binary cycle power plants have a thermal efficiency of 10-13%) (DiPippo, 2008).

Deducted total mass flow of the wells is 443 kg/s to produce approximately 14.5 MW_e electricity.

According the study done by International Finance Corporation, member of World bank Group, in June 2013 (IFC, 2013), the average capacity of 1087 wells is 3 MW_e. The deducted number of wells is 5 with a 14.45 MW_e electricity production. The total dissolved solids of all hot springs in Lake Abhe geothermal area have a range from 1700-3400 mg/L. All hot springs are alkaline and the water has been classified as Na-Ca-Cl type.

3. MODELLING OF ENERGY CYCLE

3.1 Binary geothermal power plant technique

Binary geothermal systems are suitable for medium temperature range 85-180°C (Dickson and Fanelli, 2003). Figure 14 shows a schematic diagram of ORC plant. This system uses secondary working fluid, which is operated through a thermodynamic cycle where working fluid is evaporated and condensed. Working fluid is chosen that has lower boiling point than steam and high vapour pressure at low temperature. The main components of a binary plant are:

- Preheater;
- Evaporator;
- Turbine and generator;
- Condenser and
- Feed pump.

Geothermal fluid enters the binary cycle, through heat exchanger where working fluid is heated and vapourized, and vapour will drive the turbines. Different technologies are available for binary cycles, with different working fluid in the system dependent on the well temperature. Common cycles are Organic Rankine Cycle and Kalina Cycle. Organic Rankine Cycle (ORC), uses organic working fluid, while Kalina Cycle, uses a non-organic fluid Rankine cycle, using water-ammonia mixture as a working fluid (Dickson and Fanelli, 2003).

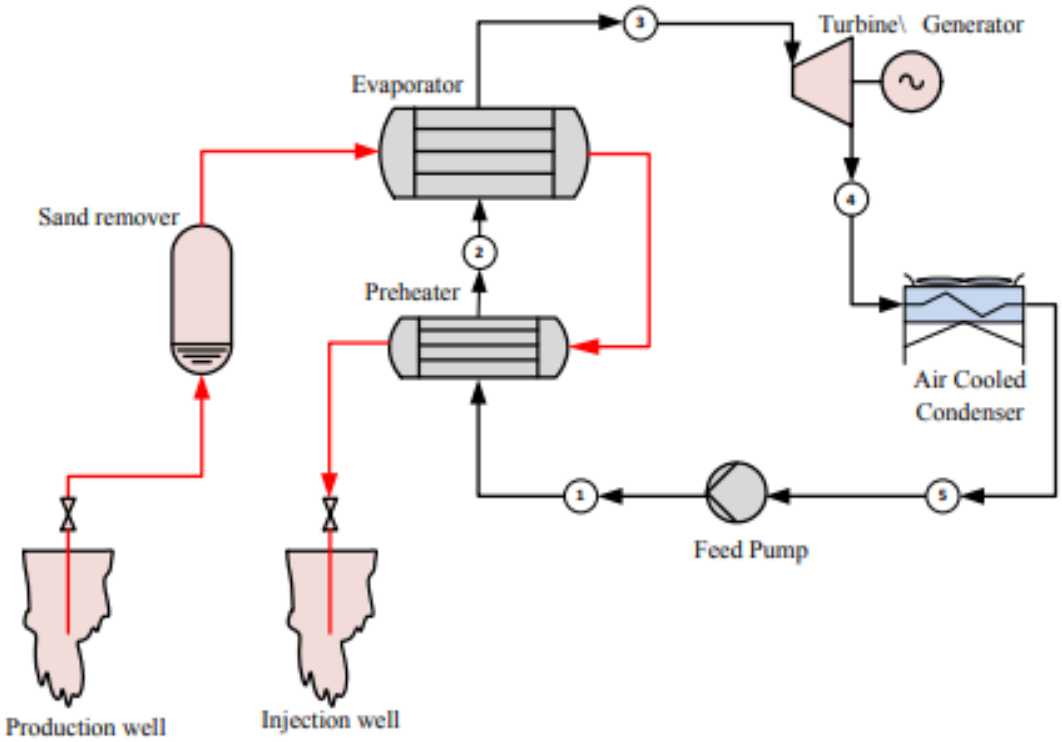

FIGURE 14: Schematic diagram of ORC plant (Ahangar, 2012)

3.2 Project methodology

In this study, binary energy cycle is chosen, since that is best fitted with the medium temperature range available and as it has a small scale of emissions. The main environmental problems concern is the release of gases and the disposal of some geothermal fluids (National Geographic, 2016).

Binary power plant is planned to be placed at the located area with five production wells and two injection wells. The geothermal power plant will work on ORC (Organic Rankine Cycle). The selection of the working fluid will be evaluated; the suitable working fluids should be taken in the consideration on the system performance analysis with a screening criteria based on the maximum net power output, thermal efficiency and specific power output SPO. Power plant operation lifetime is set to be 30 years. As DiPippo suggested, the system must be so designed to perform satisfactorily for at least 25–30 years to be deemed economically viable (DiPippo, 2008).

Resource assessments provided us with information about reservoir data such as; total flow rate, reservoir temperature and pressure, and the expected total power generation. The lack of subsurface data in Lake Abhe geothermal Field forced us to assume some crucial data. To determine unknown states of the geothermal fluid at the drilling wells planned for the project, estimation of such a character needs to be done within the ranges studied in the aforementioned literature. Values of temperature, mass flow and depths have been chosen randomly within the assumed range by using so-called Rand-between function in Microsoft Excel program.

Table 6 shows number of wells, depths of wells, estimated temperature (the wells are considered as isothermal), mass flows (values based on literature review) and pressure values. Number of reinjection wells for the process were estimated to be two with depth of 1000 m each.

TABLE 6: Wells data

Well no.	Reservoir T [°C]	Wellhead T [°C]	m [kg/s]	Wellhead pressure [bara]	Depth [m]	Enthalpy [kJ/kg]
LAPW1	142	142	88	5	1655	597,8
LAPW2	140	140	83	8	1984	589,4
LAPW3	156	156	106	7	1693	658,2
LAPW4	123	123	90	5	1521	516,8
LAPW5	168	168	76	9	1976	710,4

Geothermal binary power plants are composed into three technical systems: the geothermal fluid cycle, the power conversion cycle and the cooling system. Our challenge in designing and operating geothermal binary power plants is to manage the efficient and reliable interaction of these technical subsystems in Labe Abhe geothermal area with a hot arid climate.

The modelling and the simulation of the model consist to perform the system when some inputs (Wet-bulb temperature, cooling water supply system, etc…) conditions change in order to optimize the electrical power production process. The simulation and technical analysis were performed by EES program (F-Chart, 2016).

3.3 Process flow diagram

Overall energy process flow diagram is shown in Figure 15. The process commences at the five productions wells from LAPW1 to LAPW5. Geothermal fluid exits the wells at conditions described by states 1 to 5 respectively. The fluid passed through the wellhead valves that are used to regulate mass flow and pressure if needed. After that, the five flows are collected to the common pipe reaching the same pressure and temperature (state 6). The geothermal brine enters the system through two stages in the heat exchanger, the first stage is the evaporator and the second is the preheater. The geothermal fluid cycle (red in the Figure 15) and the working fluid cycle (blue in Figure 15) are separated, so only the heat transfer takes place through the heat exchangers.

The preheater is a heat exchanger that heats the working fluid before it enters the evaporator. Heat is added to evaporate the working fluid to its saturated vapour state (state 10) in the evaporator. Saturated vapour is then transported through the valve, enters the turbine and expands to reach the set exhaust pressure, the pressure drop between state10 and state 11 is neglected. At state 12, the working fluid

passes through the air-cooled condenser ACC and rejects the thermal energy to the open air cooling cycle (state 20-21) fed by the fans. Organic working fluid leaves the condenser at slightly sub-cooled state and passes through the feed pump (process 13-14). It raises the pressure from condenser pressure up to the high-pressure level in the station 14. The working fluid reaches its original vapourization pressure as it enters the heat exchangers and the cycle restarts. Geothermal fluid that has given away part of its thermal energy to the working fluid of the binary cycle leaves the heat exchangers at the state 8.

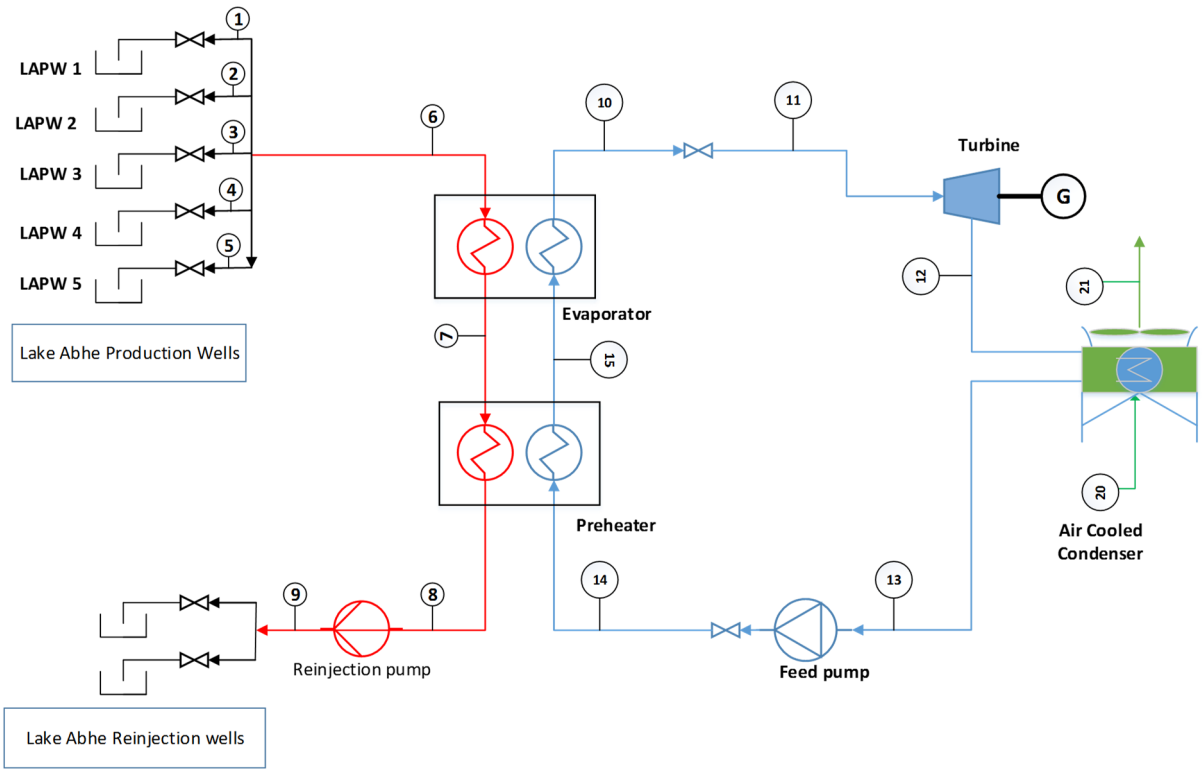

FIGURE 15: LAGF project process flow diagram

Because the fluid is at this point assumed to have still a potential of recoverable thermal energy that could be used for heating purposes. Geothermal fluid at state 9 is then split to two streams of the same mass flow and directed to the re-injection wells. Before the geothermal fluid is re-injected, it is passing through the re-injection pumps.

The following sections will provide detailed description of the processes within each of the main components of the cycle. The fundamental properties, assumptions and relations between the variables are going to be shown. These relations are presented in a form of equations on which the EES program model is constructed.

3.4 Evaporator and preheater

Heat exchangers are devices that facilitate heat transfer from hot fluid to cold fluid. Figure 16 shows the flow diagram of the heat exchanger. In order to establish the thermodynamic relationship between the geothermal fluid and the working fluid, we assume that it is in steady-state

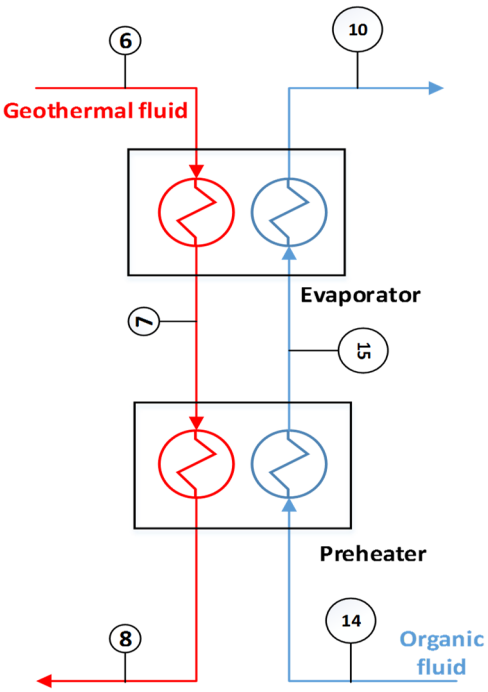

FIGURE 16: Preheater and evaporator

operating conditions and that the differences in the entering and leaving potential energy and kinetic energy are negligible.

The heat losses through the heat exchanger are neglected, so that all the heat transfer is between the geothermal fluid and the working fluid. The total amount of heat, Q added to the working fluid is equal to the heat extracted from the geothermal fluid. The following equations describe this:

$$\dot{Q} = \dot{m}_6(h_6 - h_8) \quad \textit{(kJ/s)} \quad (7)$$

$$\dot{Q} = \dot{m}_{14}(h_{14} - h_{10}) \quad \textit{(kJ/s)} \quad (8)$$

where $\dot{m}$ = Mass flow (kg/s);
h = Enthalpy (kJ/kg);
$\dot{Q}$ = Thermal energy.

Hence the thermodynamic heat balance is:

$$\dot{m}_6(h_6 - h_8) = \dot{m}_{14}(h_{14} - h_{10}) \quad (9)$$

If temperatures and heat capacity are used instead of enthalpy, which is only allowed for constant heat capacities like for fluid water but not for phase exchange in the working fluid, the left-hand side of the Equation 9 becomes:

$$\dot{m}_6 C_p(T_6 - T_8) = \dot{m}_{14}(h_{14} - h_{10}) \quad (10)$$

where C_p is the average specific heat of the geothermal fluid (kJ/kg-°C);
T_6 *and* T_8 are the inlet and exit brine temperatures (°C), respectively.

Pre-heater: $$\dot{m}_6 C_p(T_7 - T_8) = \dot{m}_{14}(h_{15} - h_{14}) \quad (11)$$

Evaporator: $$\dot{m}_6 C_p(T_6 - T_7) = \dot{m}_{14}(h_{10} - h_{15}) \quad (12)$$

The mass balance across the primary and secondary cycle in the evaporator and preheater then becomes:

The relationship which governs the temperatures at the station 7 and 15 is given in respect of the pinch as follows:

$$T_7 = T_{15} + T_{pinch} \quad (13)$$

where T_{pinch} is the heat exchanger pinch temperature difference (°C).

The pinch temperature is the smallest difference in temperature that can be reached between the primary fluid temperature and the secondary fluid temperature (DiPippo, 2008) and is usually provided by the manufacturer of the heat exchanger (Figure 17). The heat exchangers surface area between the two fluids can be determined from the basic heat transfer relationship:

$$Q = \overline{U} * A * LMTD \quad (14)$$

where U = Overall heat transfer coefficient (W/m^2.°C);
A = Total heat transfer area (m^2);
LMTD = Logarithmic mean temperature difference (°C).

LMTD can be calculated as follows:

$$LMTD = \frac{(T_{hot,in} - T_{cold,out}) - (T_{hot,out} - T_{cold,in})}{\ln \frac{(T_{hot,in} - T_{cold,out})}{(T_{hot,out} - T_{cold,in})}} \quad (15)$$

where the subscript "*hot"* refers to the fluid with a higher temperature, "*cold"* refers to the fluid with a lower temperature and subscripts "*in"* and "*out"* suggest the inlet and outlet of the heat exchanger.

According to (Ahangar, 2012) the overall heat transfer $\overline{U}$ coefficients for heat exchangers are assumed:

$\overline{U}$ =1600 W/m^2.°C for evaporator;
$\overline{U}$ =1000 W/m^2.°C for preheater;
$\overline{U}$ =600 W/m^2.°C for superheater; and
$\overline{U}$ =800 W/m^2.°C for condenser.

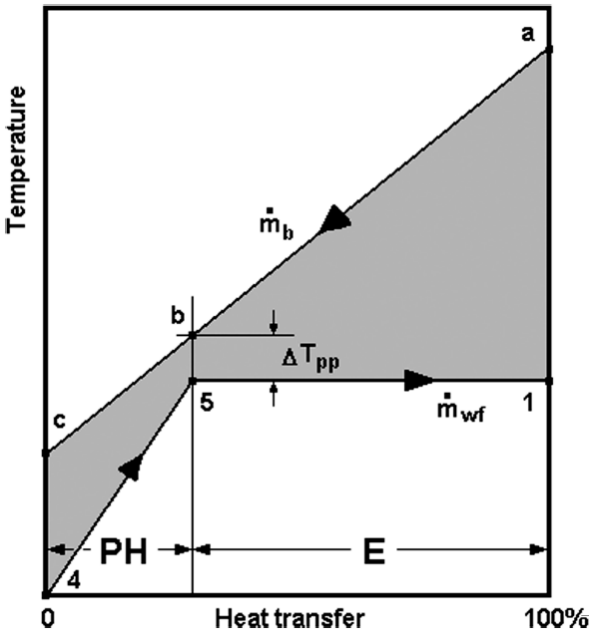

FIGURE 17: Temperature-heat transfer diagram for preheater and evaporator (DiPippo, 2008)

3.5 Turbine expansion process

The main component of the geothermal power plant is the turbine. The organic fluid coming from the vaporizer enters in the turbine (see Figure 18). The difference of pressure between the entered and the exit of the turbine creates a mechanical energy that will be transformed into electric energy through the generator coupled with the turbine. The capacity of the turbine is a fundamental factor in the design of a geothermal power plant. In an ideal turbine, the process is considered isentropic (the entropy is constant). The isentropic turbine efficiency is defined as:

$$\eta_t = \frac{h_{11} - h_{12}}{h_{11} - h_{sturb}} \tag{16}$$

The efficiency of a turbine is generally provided by the turbine manufacturer and it is usually 85% (Dickson and Fanelli, 2003). And the mechanical turbine power is defined as:

$$W_{turb,a} = \dot{m}_{11}(h_{11} - h_{12}) \tag{17}$$

The generator efficiency is at 98%. (Moon and Zarrouk, 2012) The electrical power will be equal to the mechanical turbine power times the generator efficiency:

$$W_{gen} = \eta_g W_{turb,a} \tag{18}$$

3.6 Air cooling condenser

The function of the condenser is to condense the exhaust organic fluid flowing from the turbine in order to maximize turbine efficiency by maintaining a proper vacuum by condensing the vapour form of working fluid. Condensers may be classified into two main types:

- Those in which the coolant and condensing vapour are brought into direct contact also known as direct contact condensers
- And those in which the coolant and condensate stream are separated by a solid surface, usually a tube wall, also known as Surface Condensers. The cooling air passes through a heat exchanger.

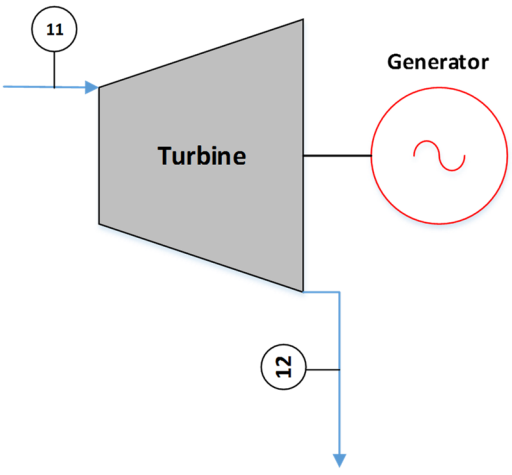

FIGURE 18: Binary turbine

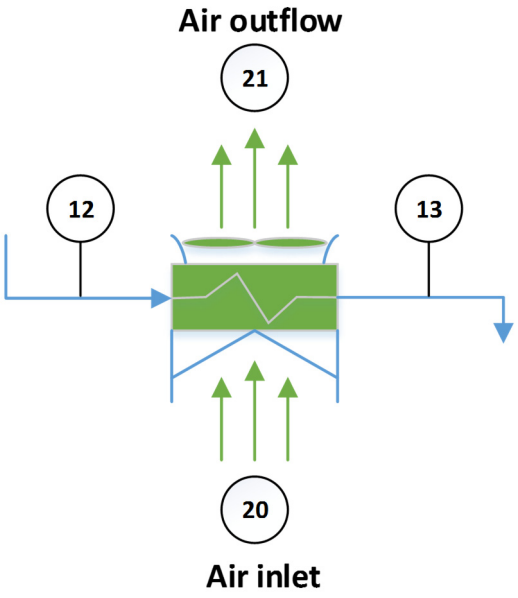

FIGURE 19: Air cooling condenser

The direct contact condenser is applicable in flash plants but not appropriate for binary plants otherwise the closed loop secondary fluid would get in contact with the coolant, which may result into environmental hazards. The operation of surface condenser is ideal for binary power plant application where secondary fluid need not to get in contact with cooling water.

In the air-cooled condensers (Figure 19), the condensing vapour flows inside a bank of finned tubes and ambient air blown across the tubes by fans serves as the coolant. Air-cooled condensers are used where water is scarce (such as desert climates) as is the case of Djibouti. However, when cooling water is available the ACC is not used because of the high parasitic load generated by auxiliary components. Their efficiency can reach up to 30% (Najafabadi, 2015) although it is lower in summer due to high dry-bulb temperature.

An energy balance for the heat exchange in the condenser gives:

$$\dot{m}_{12}(h_{12} - h_{13}) = \dot{m}_{20}(h_{21} - h_{20}) \quad (19)$$

$$Q_{cond} = \dot{m}_{12}(h_{12} - h_{13}) \quad (20)$$

3.6.1 Inlet air temperature

The temperature of Lake Abhe area summarized in Table 7. The average temperature of the twelve months is 30°C (see section 1.1). The inlet temperature is set to the average temperature of the year:

TABLE 7: Average maximum temperature

	Jan	Feb	Mar	Apr	May	Jun	Jul	Aug	Sept	Oct	Nov	Dec
Average max temperature (°C)	29	29	31	32	34	38	41	39	36	33	31	28

$$T_{avg} = T_{20} \quad (21)$$

3.6.2 Power of motor fan in air cooling condenser

The air cooled system uses electrically driven fans to cool the working fluid and is dependent on the prevailing environmental temperatures for its efficiency. To calculate the power of the fan (W) for the air cooling condenser, the equation is:

$$W_{fan} = \frac{v_{21} \cdot \Delta P_{fan} \cdot \dot{m}_{20}}{\eta_{fan} \cdot \eta_{motor}} \quad (22)$$

where ΔP_{fan} represents the drop pressure in Pa with an assumption of 150 Pa;
v_{21} is specific volume of air in m^3/s.

And, the efficiency of the fan and motor are given (Frick et al., 2015):

$$\eta_{fan} = 0.7 \quad and \ \eta_{motor} = 0.95$$

3.6.3 Power of pump

The following equation is used to calculate the power of the pump W_{pump} [kW] with a pump efficiency set at $\eta_{pump} = 0.8$ (Frick et al., 2015):

$$W_{pump} = \frac{v_{13} \cdot (P_{14} - P_{13}) \cdot \dot{m}_{13}}{\eta_{pump} \cdot \eta_{motor}} \tag{23}$$

v_{21} in the equation (22) stands for specific volume of the organic fluid in m^3/s, $\dot{m}_{13}$ is mass flow of the organic fluid in kg/s. Efficiencies of the pump and of the pump's motor are marked as η_{pump} and $\eta_{motor,pump}$, respectively.

3.6.4 Output of the power plant

The output of the power plant is found by following equation:

$$W_{auxiliary} = W_{Fpump} + W_{fan} + W_{REpump} \tag{24}$$

$$Power_{gen,net} = W_{turbine} - (W_{auxiliary}) \tag{25}$$

where *Fpump* and *Repump* refer to feed pump and reinjection pump, respectively.

3.7 Cooling tower process

Power plants invariably discharge considerable energy to their surroundings by heat transfer. The large quantities of waste heat that have been generated are often discarded in the nearby lakes or rivers. This can involve excessive heating and may disrupt life-forms. There are several methods available, most notably: Cooling towers provide an alternative in locations where sufficient cooling water cannot be obtained from natural sources. Cooling towers can operate by natural or forced convection. Also they may be counter-flow, cross-flow, or a combination of these.

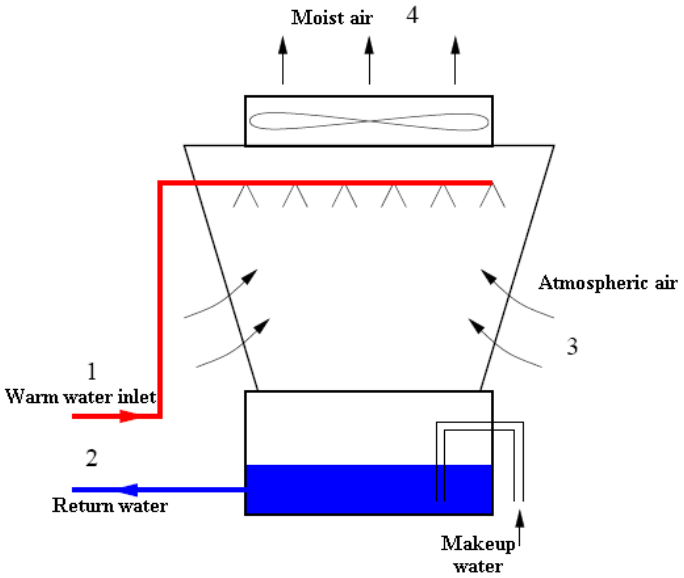

FIGURE 20: Mechanical induced draft wet cooling tower (modified from Pálsson, 2010)

We consider here air cooling forced flow cooling towers, where air is forced in counter-flow configuration against flowing water (Figure 20). The warm water to be cooled enters at 1 and is sprayed from the top of the tower. The falling water usually passes through a series of baffles intended to keep it broken up into fine drops to promote evaporation. Atmospheric air drawn in at 3 by the fan flows upward, counter to the direction of the falling water droplets. As the two streams interact, a small fraction of the water stream evaporates into the moist air, which exists at 4 with a greater humidity ratio than the incoming moist air at 3.

Since some of the incoming water evaporates into the moist air stream, an equivalent amount of water is added at 5 so that the return mass flow rate of the cool water equals the mass flow rate of the warm entering at 1. This water, in addition to compensating for evaporation and drift, keeps the concentration of salts and other impurities down.

The cooled water is collected at the bottom of the tower and pumped back to the condenser to absorb additional waste heat. Make-up water must be added to the cycle to replace the water loss due to evaporation and air draft. To minimize the water carried away by the air, drift eliminators are installed in the wet cooling tower above the spray section. The air circulation in the cooling tower used in the study is provided by fans; therefore, it is classified as a forced-draft cooling tower (Cengel and Boles, 2006).

For operation at steady state, mass balances for the dry air and water and an energy balance on the overall cooling tower provide information about cooling tower performance.
Relative humidity is denoted as:

$$\Phi = \frac{P_v}{P_s} \tag{26}$$

where P_v = Partial pressure of water vapour in the air.
P_s = Partial pressure of water vapour that would saturate the air at its temperature.

Humidity ratio is defined as:

$$\omega = \frac{M_v \Phi P_s}{M_a(P - \Phi P_s)} \tag{27}$$

where M_a and M_v =Molar masses of the dry air and the water.

The ratio of the molecular weight of water to that of dry air is approximately 0.622, this expression can be written as:

$$\omega = 0.622 \frac{P_v}{(P - P_v)} \tag{28}$$

The required mass flow rate can be found from mass and energy rate balances. Mass balances for the dry air and water individually reduce at steady state to:

$$\dot{m}_{a3} = \dot{m}_{a4} \qquad \text{(Dry air)} \tag{29}$$

$$\dot{m}_1 + \dot{m}_5 + \dot{m}_{v3} = \dot{m}_2 + \dot{m}_{v4} \qquad (Water) \tag{30}$$

The common mass flow rate of the dry air is denoted as $\dot{m}_a$.

Since $\dot{m}_1 = \dot{m}_2$, the second of these equations becomes:

$$\dot{m}_5 = \dot{m}_{v4} + \dot{m}_{v3} \tag{31}$$

With $\dot{m}_{v3} = \omega_3 \dot{m}_a$ and $\dot{m}_{v4} = \omega_4 \dot{m}_a$:

$$\dot{m}_5 = \dot{m}_a(\omega_4 - \omega_3) \tag{32}$$

Accordingly, the two required mass flow rates, $\dot{m}_a$ and $\dot{m}_5$, are related by this equation. Another equation relating the flow rates is provided by the energy rate balance:

$$\dot{m}_1 h_{w1} + \dot{m}_5 h_{w5} + \dot{m}_a h_{a3} + \dot{m}_{v3} h_{V3} = \dot{m}_2 h_{w2} + \dot{m}_a h_{a4} + \dot{m}_{v4} h_{v4} \tag{33}$$

Introducing $\dot{m}_1 = \dot{m}_2$, $\dot{m}_5 = \dot{m}_a(\omega_4 - \omega_3)$, $\dot{m}_{v3} = \omega_3 \dot{m}_a$ and $\dot{m}_{v4} = \omega_4 \dot{m}_a$, and solving:

$$\dot{m}_a = \frac{\dot{m}_1(h_{w1} - h_{w2})}{h_{a4} - h_{a3} + \omega_4 h_{v4} - \omega_3 h_{v4} - (\omega_4 - \omega_3) h_{w5}} \tag{34}$$

3.7.1 Power of motor fan in cooling tower

To calculate the power of the fan P_{fan} (W) at the cooling tower, the equation is:

$$P_{fan} = \frac{\dot{v}_{air} \Delta P}{\eta_{fan}} \tag{35}$$

and,

$$\dot{v}_{air} = \frac{\dot{m}_{air}}{\rho_{air,out}} \tag{36}$$

Thus,

$$P_{motor,fan} = \frac{P_{fan}}{\eta_{motor,fan}} \tag{37}$$

where $\mathbf{\Delta}$P = The drop pressure, in Pa;
$\dot{v}_{air}$ = The volume flowrate of air, in m^3/s;
$\dot{m}_{air}$ = The mass flow of the air, in kg/s;
$\rho_{air,out}$ = The density of the air out the cooling tower in kg/m^3;
η_{fan} = The efficiency of the fan;
$\eta_{motor,fan}$ = The efficiency of the motor of the fan.

3.7.2 Cooling water pump

The following equation is used to calculate the power of the pump P_{pump} (W):

$$P_{pump} = \frac{\dot{v}_{water} \Delta P}{\eta_{pump}} \tag{38}$$

and,

$$\dot{v}_{water} = \frac{\dot{m}_{water}}{\rho_{water}} \tag{39}$$

Thus,

$$P_{motor,pump} = \frac{P_{pump}}{\eta_{motor,pump}} \tag{40}$$

where $\mathbf{\Delta}$P = The drop pressure, in Pa;
$\dot{v}_{water}$ = The volume flowrate of water, in m^3/s;
$\dot{m}_{water}$ = The mass flow of the water, in kg/s;
ρ_{water} = The density of water in kg/m^3;
η_{pump} = The efficiency of the pump;
$\eta_{motor,pump}$ = The efficiency of the motor of the pump.

3.8 Performance metrics parameters

Specific Power Output (SPO) is given by the ratio of the net power output and the total mass flow rate of geothermal fluid with a unit of kW/(kg/s):

$$SPO_{net} = \frac{W_{gen,net}}{\dot{m}_7} \tag{41}$$

Thermal efficiency is given by the ratio of net power output and the total thermal of the system (Q_v):

$$\eta_{efficiency} = \frac{W_{gen,net}}{Q_v} \tag{42}$$

Turbine Steam rate is given by the ratio of the total mass flow rate of geothermal fluid and the net power output with a unit of (kg/s)/MW:

$$TSR = \frac{m_7}{W_{gen,net}} \tag{43}$$

3.9 Cooling systems

One of the key elements of the binary power plants is the cooling systems. The main goal of the cooling systems is to condense the vapour entering the turbine, lower the heat rejection temperature, raise power output and increase heat to power conversion efficiency. In the paper wrote by (Mendrinos et al., 2006), it is denoted there are three different cooling systems.

- The surface water system, the cooling fluid is water, which is transported to the power plant through pipes from a river, a lake or the sea. It is also known as once-through cooling system; use a water's cooling capacity a single time. These systems use large volumes of water and typically discharge the once-through water directly to waste in the environment.
- Wet type cooling tower uses both water and air with a cooling tower see details in the Section 3.7 as well as the cooling tower that was choosing for this study.
- Dry cooling system is explained in the Section 3.6 and a schematic diagram for a dry cooling system is as shown in Figure 19.

3.10 Scaling consideration

The silica mineral deposition from geothermal brine within steam-field and generating equipment is a common problem in geothermal power production (Figure 21). During the flash process to generate additional steam from the geothermal fluid, an increase in the silica concentration of the remaining fluid (brine) appear. This silica can build up a layer of solid deposit on the internal surfaces of pipelines, flash plants and turbines, impeding the flow of the fluid and leading to a drop in conversion efficiency and high maintenance cost.

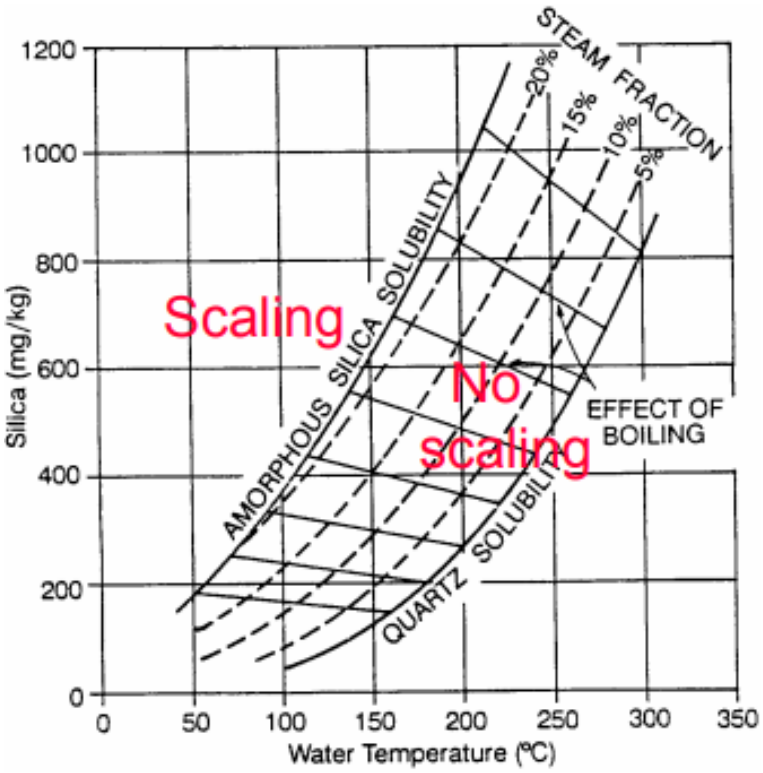

FIGURE 21: Solubility of silica in water
(Gunnlaugsson et al., 2014)

In a binary system, the geothermal fluid cools down by passing through the heat exchangers. Thereby, silica is inclined to precipitate and form a scale on the inside of the pipes. This is a basic mechanism by which scale might form in any heat exchanger. The scale that forms by this process in the heat exchangers at Wairakei is remarkable in its extreme roughness (Woodhurst, 2011).

Hence, there are two major operational impacts of this scaling process; it imposes the need for frequent cleanings of the heat exchanger tube system and - because of the decrease in flow through the system - it decreases the amount of power that can be generated (Woodhurst, 2011).

According to (Gunnlaugsson et al., 2014) a silica "rule of thumb" may say that it is only possible to cool the geothermal water by some 100°C without the risk of scaling for any given geothermal reservoir temperature. The geothermometer indicates a reservoir temperature of 176°C in LAGF. The reinjection temperature should be above of 76°C. The best choice is not be too close to this limit of scaling potential temperature. In that consideration, the reinjection temperature in our case is set at 90°C.

3.11 Working fluid selection

Many papers have treated the choice of the working fluids using simulations of the thermodynamic models. A review of the scientific literature in the field of working fluid selection was proposed by the authors in (Quoilin, et al., 2011). Despite the multiplicity of the working fluid studies, no single fluid has been identified as optimal for the ORC. The performance of a binary-cycle geothermal power plant obviously depends upon the thermodynamic properties of the secondary working fluid used in the binary circuit. The working fluid must be carefully selected based on the thermodynamic specifications, safety, environmental and economy aspects (DiPippo, 2008).

In our case, the pre-screening criteria is based on well-known fluids that are used in the operating ORC plants or that has been studied on the literature. Hydrocarbons such as pentanes or butanes and refrigerants such as R245fa are good candidates for moderate and low temperatures typically lower than 200°C (Quoilin et al., 2011).

The final selection of working fluid candidates is described in Table 8; where their relevant thermodynamic properties is shown and pure water is included for comparison. These include flammability, ozone depletion potential (ODP) and global warming potential (GWP). The GWP is considered to be relative to the amount of heat that can be trapped by similar mass of carbon dioxide as the working fluid being analyzed (DiPippo, 2008). All of the candidate fluids have critical temperatures and pressures far lower than water. The suitable working fluids should be taken in the consideration on the system performance analysis. The screening criteria are maximum net power output, thermal efficiency and specific power output SPO.

TABLE 8: List of considered working fluids

Fluids	Critical temperature (°C)	Critical pressure (bar)	Flammability	ODP	GWP	Molecular weight (g/mol)
R245fa	154.1	36.51	Non-flammable	0	950	134
Isobutane	134.7	36.4	Very high	0	3	58.12
Isobutene	144.9	40.1	Very high	0	3	56.11
Isopentane	187.2	33.7	Very high	0	3	72.15
N-pentane	196.5	33.64	Very high	0	3	72.15
Toluene	318.6	41.26	Very high	0		92.14
Water	374	220.6	Non-flammable	0	-	18.02

In the present case of the ORC, the thermodynamic optimization aims at maximizing the net power output. This is equivalent to maximizing the overall efficiency since the flow rate and the temperature of the heat source are fixed. For the purpose of this optimization, the pinch points on the heat exchangers must be imposed. A value of 5.4 is selected for both the condenser and the evaporator. The pressure drop is neglected on the evaporator and on the condenser. And the temperature of condenser is kept constant at 40°C. In the air cooling condenser, the temperature of the air is higher than 25°C resulting in condensing temperatures around 40-50°C (Mendrinos et al., 2006). For this reason, the condenser temperature is assumed at 40°C for the selection of the working fluid. This was done for simplification of the model.

This analysis was conducted for each candidate working fluid in order to define maximum net power output, thermal efficiency and SPO of the ORC as well as the optimum evaporation temperature. The

results of this optimization are presented in Table 9 and in the Figures 8 and 9. Isobutane is the fluid showing the highest overall efficiency, followed by Isobutene and R245fa. These two hydrocarbons have the maximum parasite load. The evaporating temperature of the latter are close to their critical point. It is therefore obvious that these two fluids are not suitable for the present heat source temperature. R245fa has the maximum power output and specific power output (SPO). R245fa is best fit to our model.

TABLE 9: Performance of the different working fluids

Fluids	T of HX (°C) (at State 10)	Efficiency [%]	Net power (kWe)	SPO (kWe/ (kg/s))	Parasite load (kWe)
Isopentane	107.7	11.81	7740	17.54	4619
Isobutane	118.7	13.01	7908	17.85	5702
N-pentane	106.4	11.71	7711	17.41	4536
R245fa	111.5	12.28	7979	18.01	4873
Toluene	98.05	11.49	7735	17.46	4286
Isobutene	112	12.64	7952	17.95	5276

Figures 22 and 23 illustrate the net power output curves of 6 working fluids in the function of the temperature.

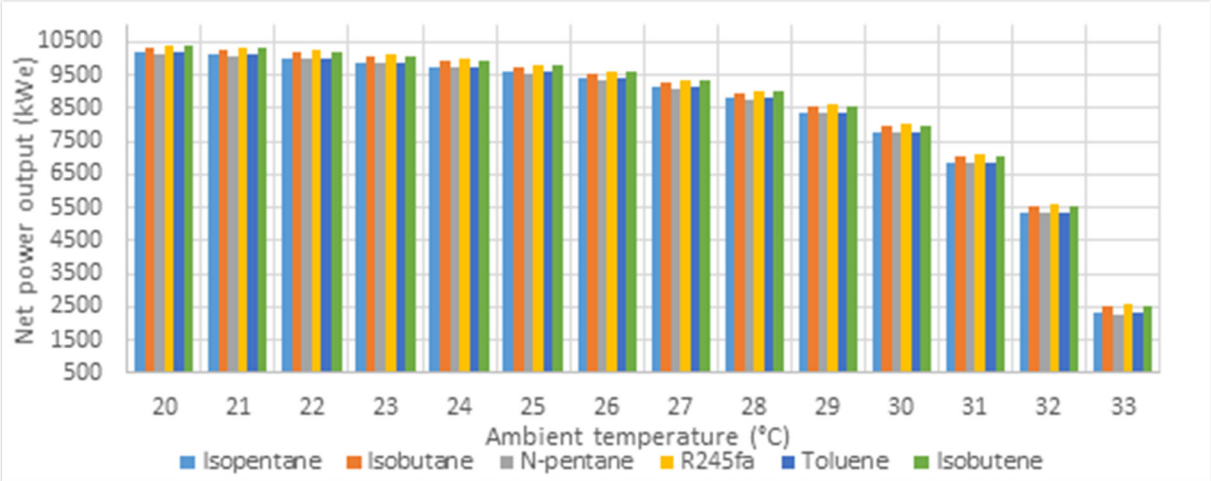

FIGURE 22: Comparison of net power output for six working fluids in an ACC system

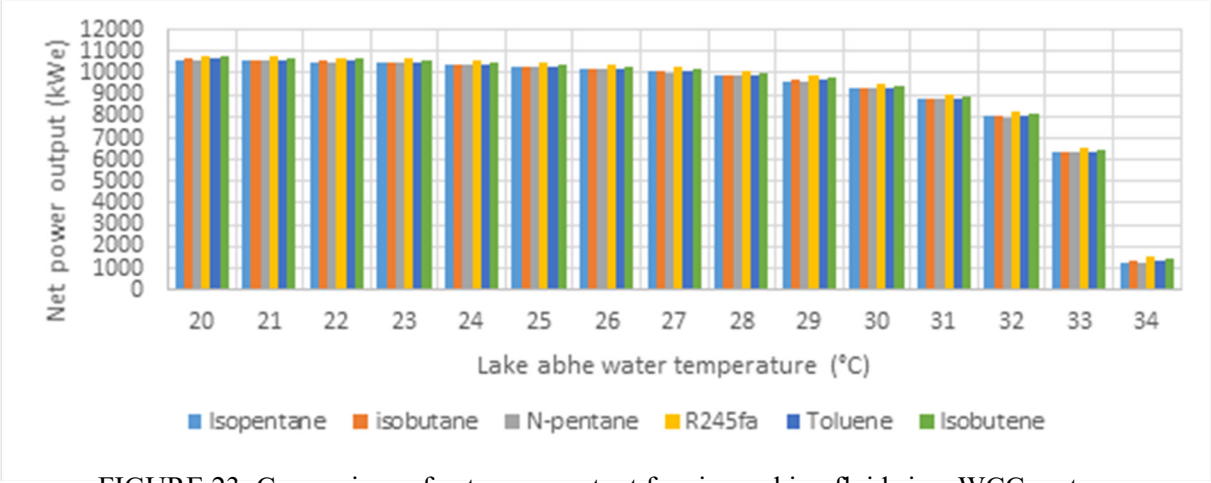

FIGURE 23: Comparison of net power output for six working fluids in a WCC system

In Figures 22 and 23 when the temperature goes up the net power output decreases. In the basic binary plant with an air cooled condenser and with water cooling condenser, the both option the curves have the same trend. The R245fa has the maximum net power output.

3.12 Modelling of scenarios and results

3.12.1 Dry cooling system

Implementation of an air-cooled binary geothermal power plant in southern Djibouti is studied. The current performance of the plant is analysed with an emphasis on the effects of seasonal climate changes. Table 10 summarizes the common boundary of the basic binary plant with air-cooled condenser simulation.

TABLE 10: Common boundary conditions for the models

Parameters	Value	Units
Working fluid	R245fa	
Geothermal fluid temperature	145.7	°C
Average temperature of LAGF	30.04	°C
Geothermal fluid pressure	5	bar
Geothermal fluid flowrate	443	Kg/s
ΔPfan	150	Pa
Fan Efficiency	70	%
Motor efficiency	95	%
Turbine efficiency	85	%
Generator efficiency	98	%
Preheater heat transfer coefficient	1000	$W/m^2.°C$
Evaporator heat transfer coefficient	1600	$W/m^2.°C$
Condenser heat transfer coefficient	800	$W/m^2.°C$

Dry cooled binary plants highly depend on local ambient temperature hence subjected to efficiency fluctuations as the temperature changes both daily and seasonal. On a hot summer day, production can drop down to 50% because of insufficient cooling (VERKÍS, 2014). When this type of cooling system is preferred, the fluctuations in ambient temperature need to be considered.

Optimum condenser temperature

The goal is to find the condenser temperature that maximizes the net power output. The ambient temperature is set at 30.04°C that represents the average temperature in Djibouti. The Figure 10 shows the net power output in function of temperature of the condenser. The optimum power output is about 8798 kWe and occurs at a condenser temperature of 46ºC. It is pointed out in Figure 24 by a black circle.

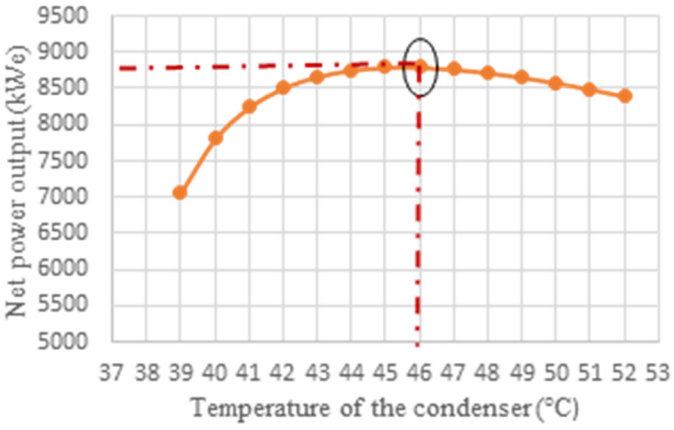

FIGURE 24: Optimum temperature of the condenser

Keeping the condenser temperature at 46°C, and ranging the average maximum ambient temperature in Djibouti from 28 to 41°C temperature as described in the section 1.2; a calculation of the net output power have been done and are shown in the Figure 25. The highest temperatures in the summer have a null net power output with this condenser temperature kept

at 46°C. There is no production in the summer, which means there is no income. For that purpose, the temperature of the condenser has been slightly raised to 50°C in order to have non-zero net power output in the summer (Figure 26). Even if the temperature for each month decrease comparing with the 46°C condenser temperature model but for the overall net power output of the 50°C has a higher total energy produced yearly, respectively 55.3 and 64.4 GWh (see Table 11).

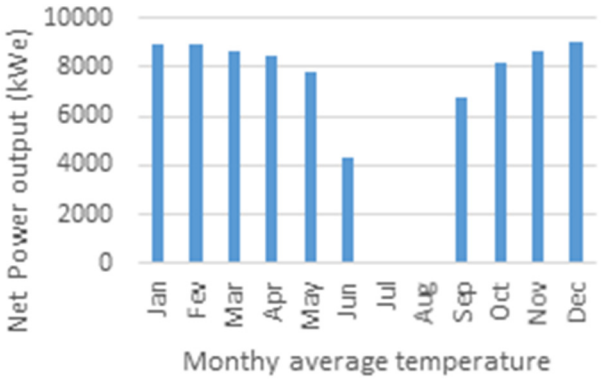

FIGURE 25: Power output over the year with 46°C condenser temperature

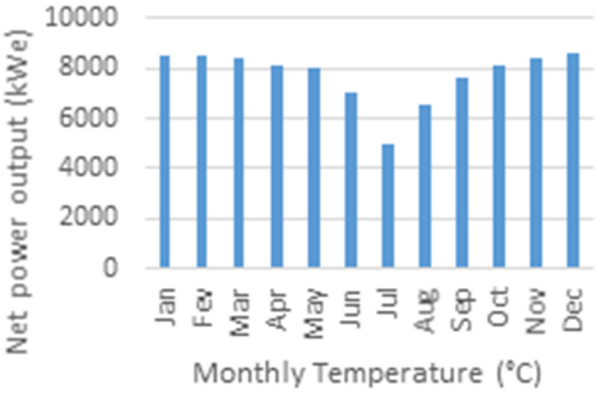

FIGURE 26: Power output over the year with 50°C condenser temperature

TABLE 11: Comparison of the model with two different condenser temperature

Cond. T°C	Jan (kWh)	Fev (kWh)	Mar (kWh)	Apr (kWh)	May (kWh)	Jun (kWh)	Jul (kWh)	Aug (kWh)	Sep (kWh)	Oct (kWh)	Nov (kWh)	Dec (kWh)	Average (GWh)
46°C	8946	8946	8635	8427	7834	4277	0	0	6767	8168	8635	9066	64.4
50°C	8544	8544	8373	8146	8002	7011	4969	6557	7617	8146	8373	8614	55.3

The Figure 27 depicts our model with the air-cooling condenser, using R245fa as a working fluid and a fixed pinch temperature set at 5.4°C. The model was done with the average annual temperature in Djibouti (30.04°C). The net power output obtained is 8461 kW_e with an efficiency of the plant at 10.44%.

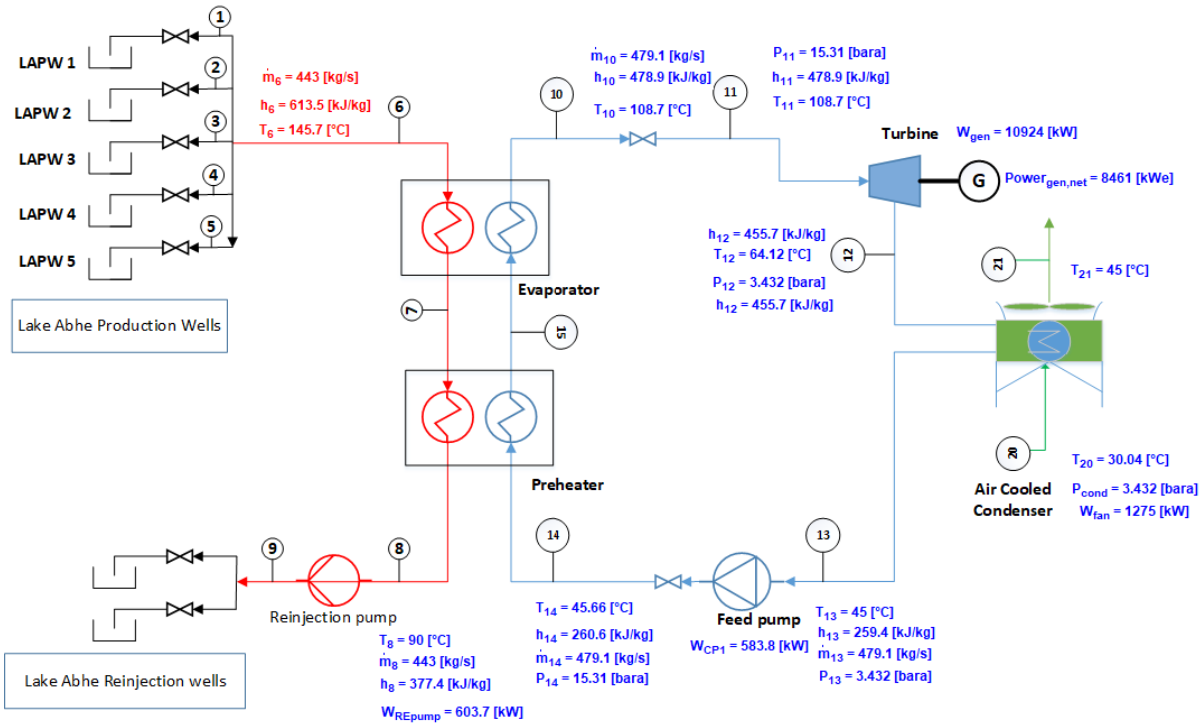

FIGURE 27: Schematic of the power plant with ACC

Dry cooling system is best suitable for areas where there is water stress or where strict water regulations prevail. However, the major problem faced by many standalone geothermal power plants, particularly in hot and arid climates such as Djibouti, is the adverse effects of temperature change on the operation of air-cooled condensers, which typically leads to fluctuation in the power output, and degradation of thermal efficiency. In the summer, the production drops down to 42% because of insufficient cooling.

3.12.2 Water cooled condenser

Lake Abhe water temperature ranges between 22 and 34°C, the calculations of the output power have been done and are shown in Figure 28. The net power output of the water-cooling condenser decrease when the temperature of the Lake Abhe water increase. On the contrary, the quantity of the water from the Lake using to cool the plant increase when the temperature of the Lake goes up.

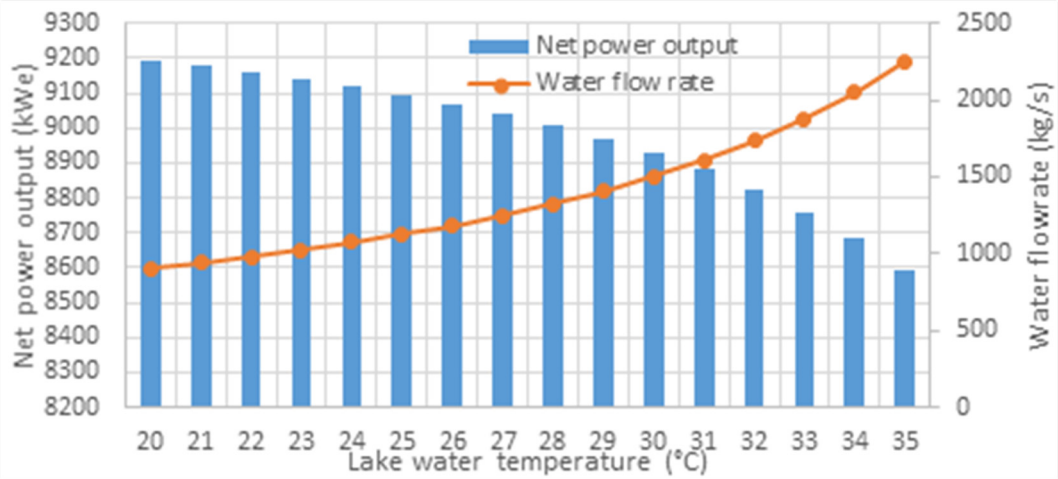

FIGURE 28: Power output of the plant with a water-cooled condenser

Figure 29 depicts our model with a water cooling condenser, using R245fa as a working fluid and a fixed pinch temperature set at 5.4°C. The model was done with the average annual temperature of the lake Abhe water in Djibouti (28°C).

The net power output of air cooled condenser calculated with the annual average ambient temperature is 8461 kW_e, when the net power output of the water cooling plant calculated with the annual average temperature of Lake Abhe water is 9007 kW_e. Comparing the two methods the net power output increase 6.1% for the benefit of water cooling condenser. The Lake Abhe water quantity is estimated approximately at 3 billion tons (Hughes and Hughes, 1992). However, the required amount of water for this case is calculated to be about 1324 kg/s that means 41.8 million tons per year corresponding 1.4 % of the total lake water. These systems draw energy out of the working fluid before expelling the water back into their original source. In addition, the temperature of water going back to the lake has gain a 17°C more.

This is the most energy efficient way to cool the working fluid as nature is supplying most of the energy required to move the water, however this deviates a large amount of water which disrupts and damages the local aquatic ecosystems through excessive withdrawals and thermal pollution.

3.12.3 Wet type cooling tower

The cooling tower systems initially draw water from a source but once it is in the system it is stored in a water tower. This tower exposes the water to air allowing it to cool before it cycles through the condenser. Some of the water is lost due to evaporation at the water tower which needs to be replaced; the only time additional water is drawn from the source. Using the closed loop system allows a plant to be totally self-contained and doesn't require a moving water source. Here, the term of "cooling tower"

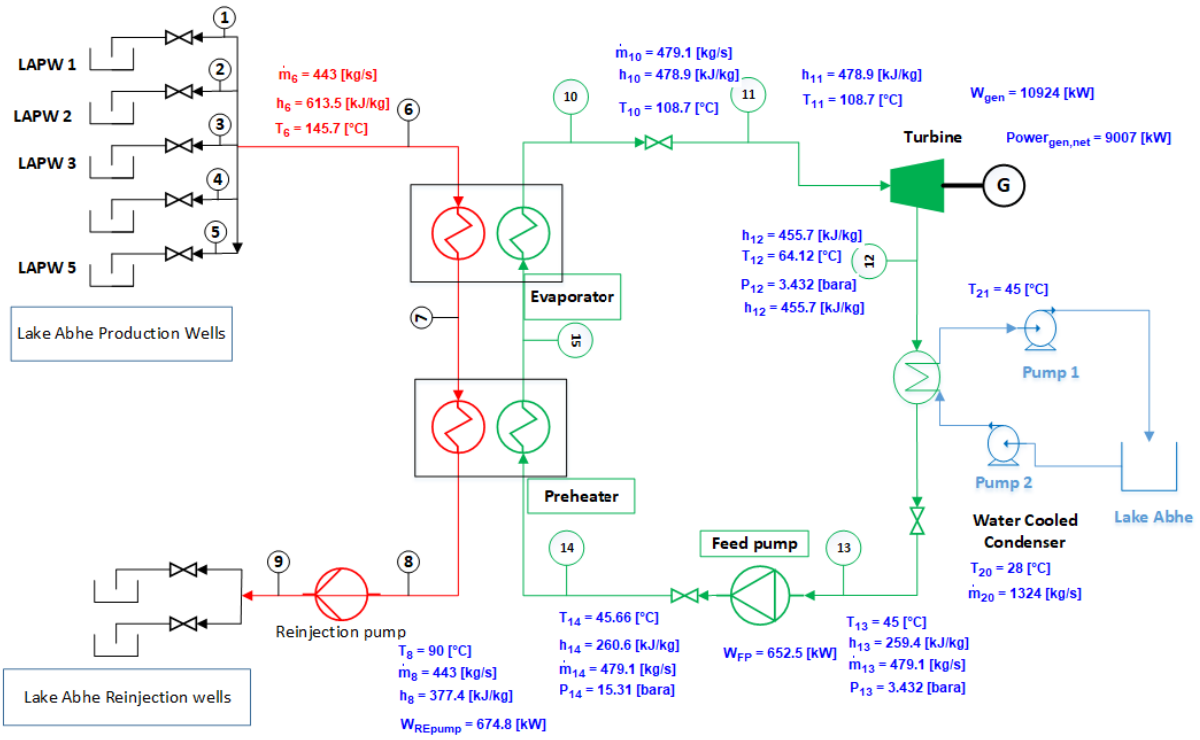

FIGURE 29. Schematic of the power plant with WCC

is used through misuse language; it is normally a water cooling condenser with cooling tower. Table 12 summarizes the common boundary of the basic binary plant with wet type cooling tower simulation.

TABLE 12: Common boundary conditions for the models

Parameters	Value	Units
Working fluid	R245fa	
Geothermal fluid temperature	145.7	°C
Average temperature of LAGF	30.04	°C
Geothermal fluid pressure	5	bar
Geothermal fluid flowrate	443	Kg/s
ΔPfan	150	Pa
Fan Efficiency	70	%
Motor efficiency	95	%
Turbine efficiency	85	%
Generator efficiency	98	%
Humidity ratio	65	%
Condenser temperature	50	°C
Range	10	°C
Approch	3	°C
Preheater heat transfer coefficient	1000	$W/m^2.°C$
Evaporator heat transfer coefficient	1600	$W/m^2.°C$
Condenser heat transfer coefficient	800	$W/m^2.°C$

With a wet bulb temperature ranging from 16 to 34°C, the calculations of the net power output have been done and are shown in the Figure 30. The net power output increases when the wet-bulb temperature of Lake Abhe decreases. With a wet bulb temperature above 33°C the plant does not function.

Djibouti being among of the country are classified as hydric stress water. As a result, air-cooling is the best suitable option for satisfying the cooling demands of geothermal power where there is water stress (or where strict water regulations prevail). However as seen in the above paragraph the temperature change in particularly in summer caused that the excess heat of the power due to high ambient temperature cannot be reject. That conduct a low efficiency. One of the most effective approaches to reduce the cost of electricity generation and improve efficiency is the hybridization of different renewable technology (Zhou, 2014). Solar and geothermal energy resources are of particular interest in Djibouti for hybridization due to their wide availability and the vast reserves.

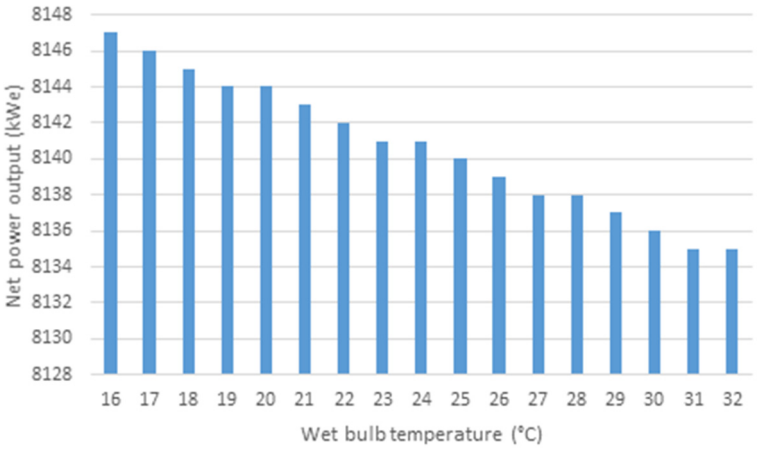

FIGURE 30: power output vs. wet bulb temperature

3.13 Solar-geothermal hybrid

With its geographical position and generally clear skies, Djibouti benefits from an important solar energy resource. The annual duration of bright sunshine is 3240 hours (ISERST, 1984). Djibouti is among the countries with a very high annual sunshine rate, citing France as its comparison, its sunstroke rate is between 1750 and 2750 hours depending on the region (Aye, 2011).

TABLE 13: Global solar average irradiation (kWh/m²/day) in Djibouti's districts

Month	Ali-Sabieh	Dikhil	Djibouti-ville	Obock	Tadjourah	Average
January	6	5.6	6.0	5.1	4.7	5.5
February	6.3	6.4	6.2	6.1	5.7	6.1
March	6.9	6.8	6.8	6.5	6.2	6.6
April	7.3	7.1	7.3	6.9	6.7	7.1
May	6.5	6.5	6.4	6.5	5.8	6.3
Jun	6.0	6.7	6.1	6.3	5.8	6.2
July	5.6	6.3	6.1	5.9	5.3	5.8
August	5.9	6.7	6.7	6.5	6.2	6.4
September	6.2	6.7	6.0	6.6	5.9	6.3
October	6.4	7.2	6.9	6.4	5.8	6.5
November	5.5	6.4	6.5	6.0	5.5	6.0
December	4.4	5.9	5.6	5.8	4.8	5.3
Annual mean	6.1	6.5	6.4	6.2	5.7	6.2

Table 13 illustrates the annual average irradiation for the five Djibouti's districts. The homogeneous availability of solar energy throughout the territory is remarkable despite some seasonal variations that occur although these variations are small.

TABLE 14: Average annual irradiation in Djibouti's districts (kWh/m²/day)

Districts	Ali-Sabieh	Dikhil	Djibouti-ville	Obock	Tadjourah	Moyenne
kWh/m²/an	2219.6	2380.9	2330.3	2268.6	2078.5	2255.6

TABLE 15: Average monthly daily sunshine duration

Months	Jan	Feb	Mar	Apr	May	Jun	Jul	Aug	Sep	Oct	Nov	Dec
Sunshine (Hours/day)	8	7.5	8.5	9	10	9.5	8.5	9	9.5	9.5	9.5	8.5

In Djibouti, the sun could provide daily more than 45 times the annual electricity needs of the country, taking into account the current technology that can recover only 13% of this energy. The country has an area of 23,200Km², the energy received daily is then 142 680 GWh (E=6,15 (kWh/m2/day)*2.32.1010 (m^2)=142 680 GWh). The average daily sunshine duration is around 8 hours.

3.13.1 Technical analysis of the hybrid solar-geothermal plant

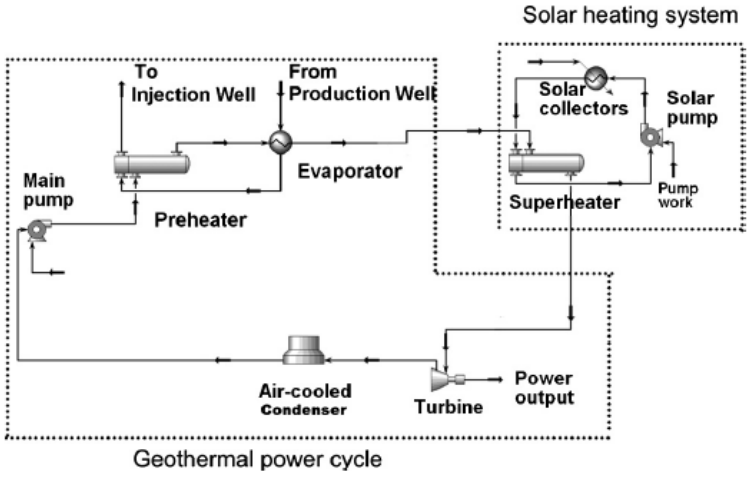

FIGURE 31: Schematic diagram of the hybrid solar–geothermal power plant (Zhou et al., 2013)

The hybrid plant consists of two parts. The first part is a geothermal ORC power cycle configured in a binary arrangement. The second is composed of a solar heating system comprising a superheater, a solar pump, and solar collectors. Figure 31 describes the hybrid plant combined the geothermal and solar plant together. As described in the paragraph 1.3, the solar heating system is installed between evaporator and the turbine. Before the ORC working fluid enter the turbine, it passes through the solar superheater unit where its temperature is further increased by the solar energy. The heat is then converted into mechanical work and ultimately electricity as the working fluid expands in the turbine unit. The air-cooled condenser (ACC) condenses the working fluid from the turbine and then a new cycle begins again. The total heat input to the hybrid solar–geothermal power plant (Qtot) was defined as the sum of the solar heat input (Q_{solar}) and the geothermal heat input (Q_{geo}).

$$Q_{tot} = Q_{geo} + Q_{solar} = m_6 \times (h_6 - h_8) + A_{solar} \times DNI \quad (44)$$

where A_{solar} is the solar aperture area, DNI is the effective solar irradiance for the solar collectors (i.e. solar direct normal irradiance).

The heat losses in the solar field largely depend on the heat loss behaviour of the Heat Collection Elements (HCEs) within the solar collectors. (Zhou et al., 2013) developed a general correlation by performing a polynomial regression of all the existing data reported in the literature on HCEs heat losses of low to high efficiency solar collectors. This correlation provides the average HCEs heat loss as a function of the temperature gradient between the ambient temperature and the solar heat transfer fluid temperature, ΔT:

$$Q_{loss} = -0.04162 \times \Delta T + 0.00448 \times \Delta T^2 - 1.43426 \times 10^{-5} \times \Delta T^3 + 2.32022 \times 10^{-8} \times \Delta T^4 \quad (45)$$

Other types of parasitic penalties in the solar field were also considered, including solar piping heat losses ($Q_{loss,piping}$), power consumption of the solar pump ($W_{pump,solar}$), and the power required to drive the collectors and electronics (W_{drive}).

$$Q_{loss,piping} = 0.01693 \times \Delta T - 1.683 \times 10^{-4} \times \Delta T^2 + 6.78 \times 10^{-7} \times \Delta T^3 \quad (46)$$

$$Q_{pump,solar} = 1.052 \times 10^{-5} MWe/m^2 \quad (47)$$

$$Q_{drive} = 2.66 \times 10^{-7} MWe/m^2 \quad (48)$$

The chosen solar heat transfer fluid in our case is Benzene with a critical temperature and pressure of 288.9 and 48.94°C, respectively. The ambient temperature range is 23-41°C, as reported in Table 1. The nominal DNI is assumed to be 1000W/m^2.

3.13.2 Results and discussions

Results of the basic model of the binary power plant with an air-cooled condenser and hybrid modelling are presented in Table 11. With a geothermal fluid mass flow of 443 kg/s and temperature of 145.7°C. The air-cooled condenser binary model produces 10924 kWe of gross power output with an auxiliary power of 22.6% of the total gross output power that the fan power represents 51.8% of the latter. The cycle efficiency is 10.44%. For the hybrid solar and geothermal power plant, the same conditions are set. The power output is 13865 kWe where 20.6% go for the use of the auxiliary components. With 10.18 as cycle efficiency, the hybrid specific power output is 12.13 kW/(kg/s).

TABLE 16: Results of the different scenarios

Parameters	Value for basic model ACC	Hybrid solar-geothermal	Units
Gross power output	10924	13865	kW_e
Net power output	8461	11014	kW_e
Auxiliary power	2463	2851	kW_e
% of Auxiliary to gross power	22.6	20.6	%
Power fan	1275	1663	kW_e
% fan in auxiliary	51.8	58.3	%
Efficiency	10.44	10.18	%
Specific Power Output (SPO)	19.1	12.13	kW/(kg/s)
Geothermal fluid flowrate	443	443	Kg/s
ORC WF mass flow (R245fa)	479.1	479.1	Kg/s
Solar WF mass flow (benzene)	[-]	465.3	Kg/s

Figure 32 depicts the net power output of the hybrid solar – geothermal and binary power plant with an air cooled condenser in function of the ambient temperature ranging from 20 to 37°C. Both curves have the same trend with a gap between the both which is reduced when the ambient temperature increases. The temperature at the condenser is kept fix to 50°C. The ambient temperature is set at 30.04°C that represents the average temperature in Djibouti. Figure 33 shows the process flow diagram of the hybrid solar-geothermal plant.

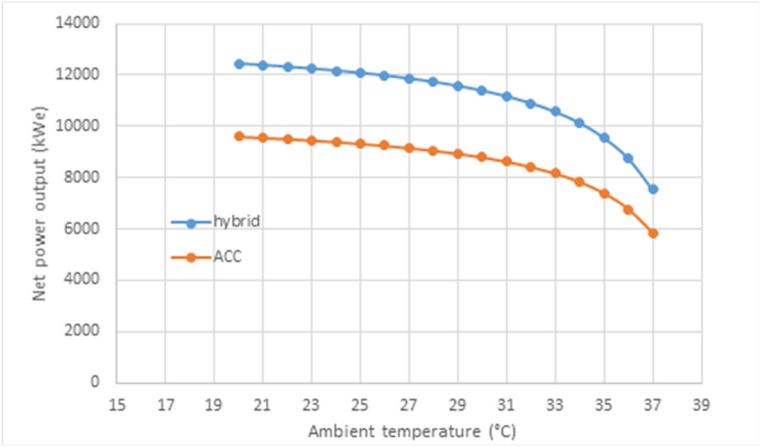

FIGURE 32: Comparison of the net power of hybrid and ACC models

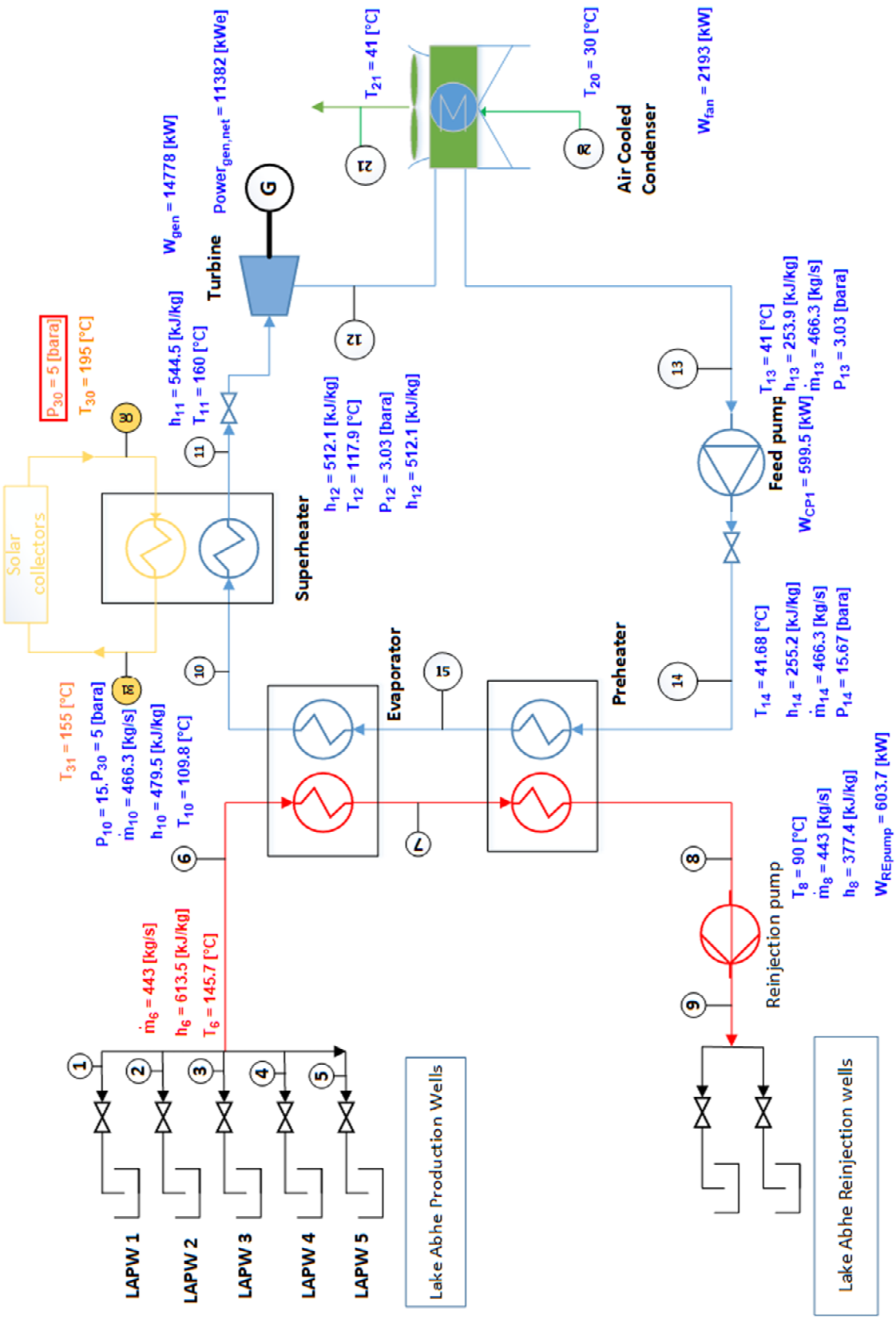

FIGURE 33: Process flow diagram of the hybrid solar-geothermal plant

4. ECONOMIC ANALYSIS

The thermodynamic analysis on its own is not sufficient to determine the viability and implementation of a particular technology. Economic consideration plays a very important role in the decision making process that govern the design of a system. Economic analysis will be performing in this section in order to assess the cost of developing the binary power plant in Lake Abhe geothermal field according of two scenarios. The scenario one is the binary power plant with air cooled condenser (ACC) and the second scenario is the concentrated solar power (CSP) combine by geothermal binary plant with ACC. The costs consist of the capital cost, operation and maintenance costs and the financial cost.

4.1 Capital costs

The capital cost are all expenses needed to put the power plant on line. These are divided in two main part; the cost of field development and cost of the power plant. For a large definition give in the paper (Bandoro and Pálson, 2010), the capital cost include the cost of the power plant and the gathering system, pipeline and pumps, pollution abatement systems and environmental compliance work, the electric sub-station and transmission line connection, civil work, engineering, legal, regulatory, documentation and reporting activities. The cost for the hybrid plant consists of cost for the geothermal plant, cost for the solar field including the HTF, and cost for Solar HX.

4.1.1 Field development cost

The field development cost consists the cost of drilling production and reinjection wells and the cost of the gathering systems (pipelines and pumps). The exploration costs are not included in the field development cost. In our case, the plan is to drill a set of 5 production and 2 reinjection wells (altogether 7 wells). At a cost of USD$ 2- 6 million per well (ESMAP, 2012), this would translate into an investment of US$ 14-42 million. Chosen the median case for this study, the total cost of the field development is assumed to be US$ 28 million.

For the hybrid plant, the cost of the field development is the sum of geothermal plant cost field development and the cost of the solar field. According to (Ayub et al., 2015) the cost of solar field is 175 €/m^2. In our study, the area of the solar field is 31,607 m^2 (A*DNI=31,607 kW with a DNI=1000 W/m^2). An average exchange rate for approximately one year (May 2017 to February 2018) obtained from the European Central Bank of 1 EURO = 1.1853 USD is used. The cost of the solar field is US $ 6,556,161. The cost of the field development of the hybrid plant is US $34,556,161.

4.1.2 Cost of the power plant

The cost of a binary power plant can be divided into three primary sections; mechanical equipment, electrical and control, and civil work (VERKÍS, 2014). A thorough breakdown of the various components can be seen in Table 17. The cost of various components of a representative binary plant are given by (Forsha and Nichols, 2018). For the nominal condition, the net power output of the scenario 1 is 8461 kW, the cost of mechanical equipment in US$/kW are summarized in the Table 17.

TABLE 17: Cost of mechanical equipment

Equipments	($/kW net power)	US$
Brine heat exchangers	135	1,142,235
Air cooled condenser	435	3,680,535
Turbine-generator	250	2,115,250
feed pump	30	253,830
Piping and valves	80	676,880
engineering	130	1,099,930
management	35	296,135
Bonds and insurance	55	465,355
contingency	150	1,269,150
profit	130	1,099,930
Total cost of the mechanical equipment	1,430	12,099,230

The costs for civil works and electrical and control equipment for a 50 MW binary power plant are US $8,351,000 and US $18,335,000 respectively (US EIA, 2013) . Using the top-down estimation and neglected the inflation, the cost for civil works is US $1,413,156 and the cost of electrical and control equipment is US $3,102,649. The total cost of the power plant is US$ 16,615,035 as summarized in Table 18.

TABLE 18: Total cost of the power plant

	Cost in USD
Mechanical equipment	12,099,230
Electrical and control equipment	3,102,649
Civil works	1,413,156
Total cost of the power plant	**16,615,035**

The total capital cost is US $44,615,035, this cost is very close to the ones that literature proposed. There are several studies that provide cost estimates for geothermal power plants based on size or electrical output. According to a publication by the Geothermal Energy Association, the average capital cost of binary projects in the United States between 2011 and 2013 was $5.18 million per MW (Geothermal Energy Association, 2014). A report published by the International Energy Agency (IEA) on geothermal project economics provides similar estimates, and includes exploration, drilling, surface facilities, and power plant costs in the capex estimation (International Energy Agency, 2010).

For the hybrid plant, the cost of the power plant is equal the cost of geothermal plant added with the cost of the solar heat exchanger. The solar heat exchanger is estimated about US $ 500,000 by (Ayub et al., 2015). That means the total cost of the plant is estimated to be US$ 45,115,035.

4.2 Operation and maintenance costs

Operation and Maintenance (O&M) consist of all aspects and activities necessary to run your power plant in a safe and most economical manner. All costs incurred during the operational phase of the power plant are called Operation and maintenance costs. Economic analysis usually distinguishes fixed and variable cost but in the case of geothermal power production, variable costs are relatively low or considered null (Bandoro and Pálson, 2010) (US EIA, 2013). An O&M agreement will help you minimize your risks and maximize your profit. The same report published by the IEA estimates O&M costs for small binary plants to be $25 /MWh.

As described in the paper (Ayub et al., 2015), the operation cost for the hybrid system is estimated by the capacity-weighted average costs of the geothermal and the solar through system as following:

$$O\&M_{hybrid} = (1 - f) \times O\&M_{geo} + f \times O\&M_{solar} \quad (50)$$

where $O\&M_{geo}$ and $O\&M_{solar}$ are the operation cost of geothermal and solar trough system, respectively. f is the solar share based on energy output.

The total O&M costs of CSP plants are to be US $ 0.025/kWh (IRENA, 2012). Or here $O\&M_{geo}$ and $O\&M_{solar}$ are equal which means that $O\&M_{hybrid} = O\&M_{geo}$.

4.3 Financial analysis

In this study, the project is considered to be financed with 30% of equity and 70% of loans. The interest rate was assumed to be 6% and the loan repayments was assumed to have a duration of about 15 years. The discount rate as its definition are thus used to attribute a value to future cash flows. In the energy sector the discount rate range from 3% to 10% approximately. A discount rate of 10% was assumed.

Geothermal production rates that in the long run exceed a reservoir's recharge rate eventually lead to reservoir depletion. Depletion of reservoir is estimated to be 1% per year in the scenario 1. In the scenario 2 the reservoir depletion is neglected according to the paper (Zhou et al., 2013) the hybridisation of solar-geothermal energy can decelerate the depletion of heat content of the geothermal reservoir overtime and hence extend its lifespan.

According to the *Presidential decree* modifying the tariffs of sale of Electric Energy and the Ancillary Fees with the reference number N°2016-199/PR/MERN, the electricity tariffs in Djibouti are in the range US $0.152/kWh – 0.309/kWh. This is based on the exchange rate USD to DJF being set at 178 - with the Djiboutian franc pledged to a fixed rate with US dollars (Goverment of Djibouti, 2018). The selling price is assumed to be US $ 0.13/kWh.

Equation 51 is used to calculate present value (PV) for project's financial model:

$$PV = \frac{C_1}{(1+r)^t} \tag{51}$$

where C_1 is the cash flow at period 1, r is rate of return, t is number of periods.

In finance, the net present value (NPV) is a measurement of the profitability of an undertaking that is calculated by subtracting the present values (PV) of cash outflows (including initial cost) from the present values of cash inflows over a period of time. Net Present Value (NPV), calculated for the financial model, becomes:

$$NPV = -C_0 + \sum_{t=1}^{T} \frac{C_t}{(1+r)^t} \tag{52}$$

where C_0 is the total investment cost, C_t is net cash inflow during the period t, r is the discount rate and t number of time periods.

Internal rate of return (IRR) is a discount rate that makes the net present value (NPV) of all cash flows from a particular project equal to zero. The higher a project's internal rate of return, the more desirable it is to undertake the project:

$$0 = \sum_{t=0}^{T} \left(\frac{C_t}{(1+r)^t}\right) - C_0 \tag{53}$$

Table 19 summarizes the main parameters for economic analysis.

TABLE 19: Main parameters for economic analysis

	Scenario 1 Binary geothermal plant	**Scenario 2 Hybrid solar-geothermal**
Net power output	8461 kW	9406 kW
Capacity factor	95%	95%
Cost development field	US$ 28 million	US $ 34,556,161
Cost of the plant	US $ 44,615,035	US$ 45,115,035
OandM	US $ 0.025/kWh	US $ 0.025/kWh
Equity	30%	30%
Selling price of electricity	13 US cents	13 US cents
Interest rate	6%	6%
Loan duration	15 years	15 years

In our case, the hybrid doesn't possess a thermal energy storage that means the CSP can add its thermal energy to the system only 8.9 hours according to the Table 10. It is equivalent to 37% of a day. The plant produces a daily sum of 37% of 11,014 kW and 63% of 8,461kW, which means 9,406 kW.

4.4 Results and discussions

The return of investment and the profit achieved are among the important indicators of the success of an engineering enterprise (Bandoro and Pálson, 2010). It is estimated that annual energy production is 70.412 GWh with 1% of degradation, and by assuming that electricity costs procured by the project are US$ 0.013/kWh, US$ 9,153,617 is generated annually with 1% of escalation. Furthermore, assuming that the project has a 30-year operating life, and discount rate of 10%, the NPV has been calculated at US $2,770,609. Figure 34 presents the cash flow and NPV for geothermal binary plant scenario of the resource under these assumptions, where the project has an IRR of 11.0%, and 24 year discounted payback period.

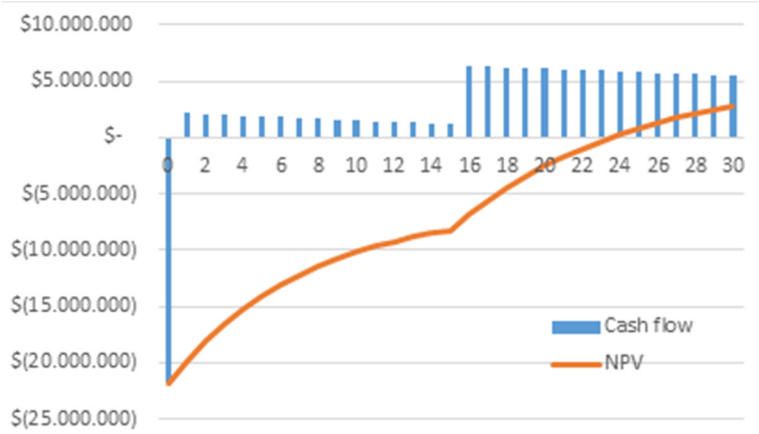

FIGURE 34: Net cash flow and NPV for scenario 1

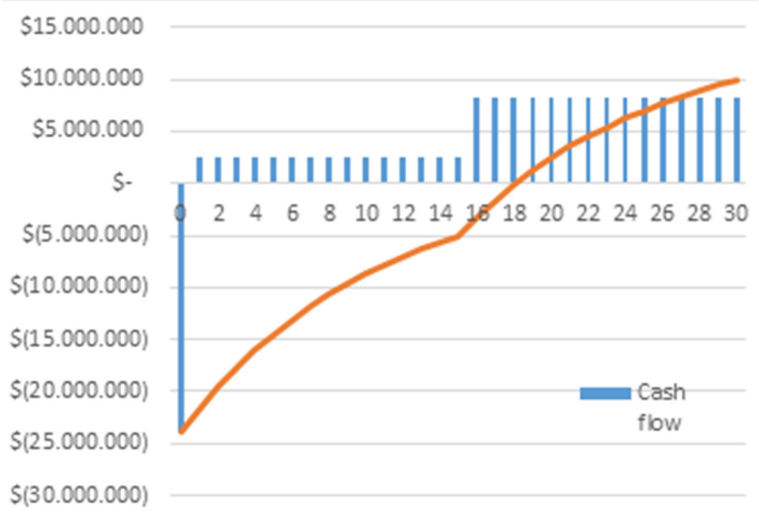

FIGURE 35: Net cash flow and NPV over lifespan

Scenario 2. It is estimated that annual energy production is 78.277 GWh without degradation, and by assuming that electricity costs procured by the project are US$ 0.013/kWh, US$ 9,153,617 is generated annually. Furthermore, assuming that the project has a 30 year operating life, and discount rate of 10%, the NPV has been calculated at US$ 9,903,231. Figure 35 presents the cash flow and NPV for geothermal binary plant scenario of the resource under these assumptions, where the project has an IRR of 13.0%, and 18 year discounted payback period.

4.4.1 Sensitivity analysis

For geothermal binary power plant standalone

Effect of various inputs on NPV as a main profitability measure for this project has been also analyzed. Figure 36 presents a sensitivity analysis in a graph with electricity prices, capital cost, reservoir depletion rate and interest rate. Each of these inputs have been varied from -50 % to +50 % of its value. Electricity prices and capital costs have the steepest lines and thus have the greatest impact on overall NPV.

Hybrid solar-geothermal plant

The impact of different parameters on the NPV was analysed in the case of hybrid plant. Figure 37 presents a sensitivity analysis in a graph with electricity prices, capital cost, reservoir depletion rate and interest rate. Each of these inputs have been varied from -50 % to +50 % of its value. The same as the scenario 1, electricity prices and capital costs have the steepest lines and thus have the greatest impact on overall NPV.

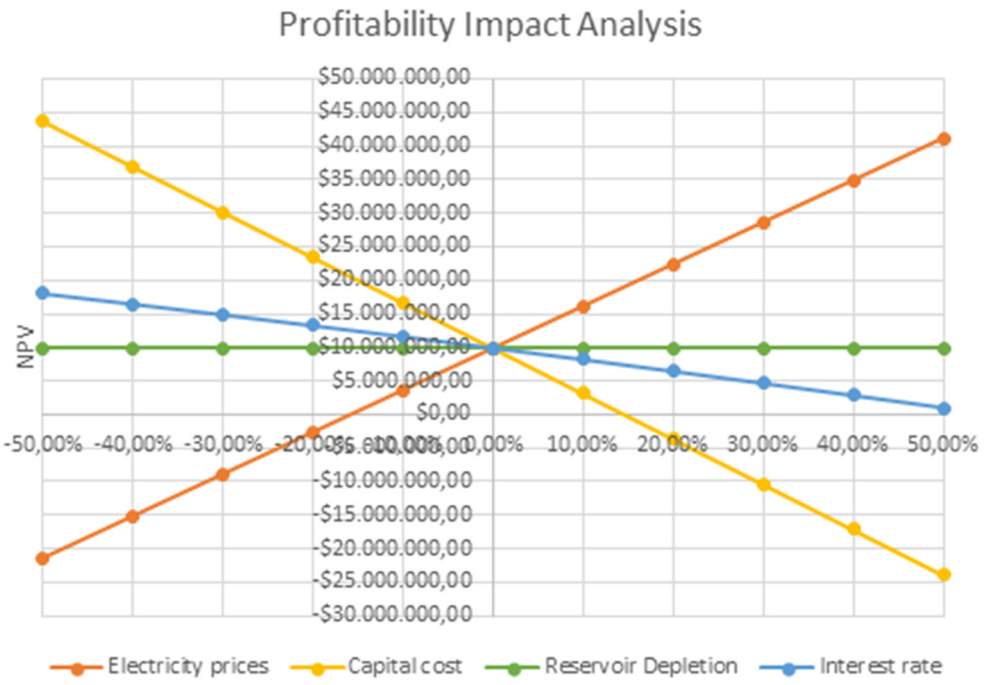

FIGURE 36: Sensitivity analysis of the NPV in scenario 1

The hybrid plant has a bigger IRR than the binary plant as advise the higher a project's internal rate of return, the more desirable it is to undertake the project. The hybrid solar-geothermal plant is the most economical use for the project, as it generates the highest NPV of the two proposed options ($9.9 m). It also has the highest IRR and quickest payback period on investment, of 13.0% and 18 years, respectively.

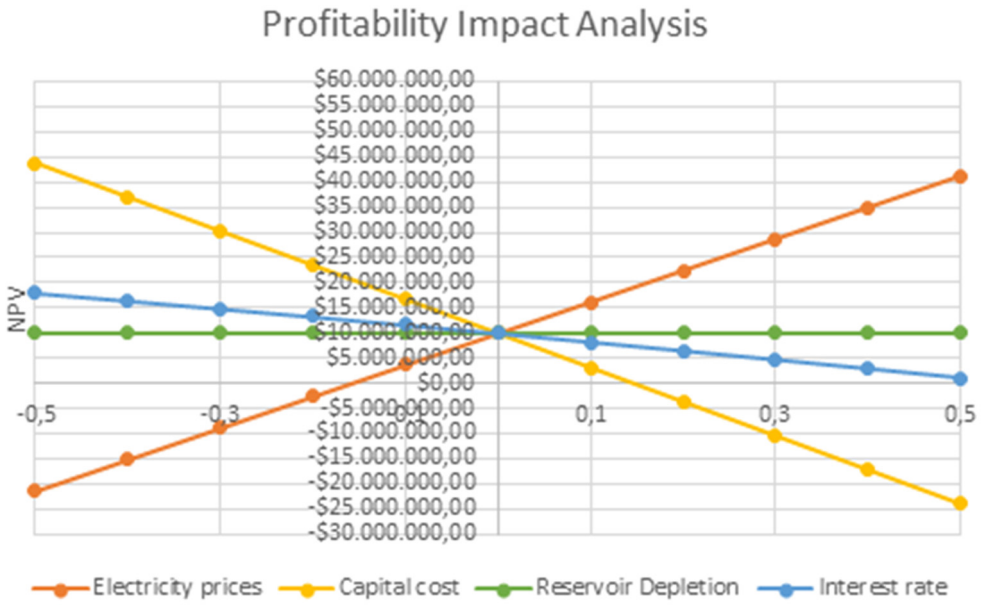

FIGURE 37: Net cash flow and NPV for the scenario 2

5. CONCLUSIONS

Djibouti lives like other African countries in a context marked by a global energetic crisis. National electricity production is based on thermal power plants running on heavy fuel oil with installed capacity of 120 MW. The energy is the common base of economic growth, increased social equity and an environment that allows the world to thrive. Without energy, there is no development. With the high cost of electricity in the country, it seemed appropriate to seek alternative energy in order to explore solar energy, wind energy, geothermal and electricity purchases from neighbouring countries via an electrical interconnection network.

For the forecasts of future demand, the peak annual demand is expected to increase up to 266 MW in 2022. Djibouti is geologically situated where two oceanic ridges (Gulf of Aden and Red Sea) meet with the East African Rift. Hence, a huge quantity of energy is dissipated from the very shallow earth mantle to the surface, the only region in the world with Iceland where an oceanic ridge is accessible on shore for geothermal exploitation. In this context, and to meet the energy challenge of tomorrow, the development of the geothermal industry becomes evident with a potential estimated to be more than 1000 MW.

Djibouti possesses several medium-enthalpy resources distributed in different parts of the country, partially situated in a hot arid zone. One of them, Lake Abhé geothermal field was recently the subject of a complete surface exploration. This was conducted by the scientists of ODDEG and ISOR jointly, with a co-financing of ICEIDA.

The objective of this paper is to determine how the medium-enthalpy resource in Lake Abhé geothermal field would be best utilized, both technically and commercially. Four scenarios, namely binary power plant with air cooled condenser, binary power plant with water cooled condenser, binary power plant with wet type cooling tower and a combined concentrated solar power and binary power plant with air cooled condenser, were examined and categorized according to their respective viability, taking into account both positive and negative external effects.

The binary power plant with water cooled condenser and binary power plant with wet type cooling tower having more than 6.1% of net power output than air cooled condenser has more negative external effects for the environments. They deviate a large amount of water which disrupts and damages the local aquatic ecosystems through excessive withdrawals and thermal pollution being rejected. Djibouti is among countries classified with hydric stress water where strict water regulations prevail, ACC was preferred than the latter.

An ACC binary plant and hybrid solar–binary were compared technically and economically. With a geothermal fluid mass flow of 443 kg/s and temperature of 145.7°C. The air-cooled condenser binary model produces 10,924 kW_e of gross power output with an auxiliary power of 22.6% of the total gross output power that the fan power represents 51.8% of the latter. The cycle efficiency is 10.44%. With the same condition, the hybrid solar-geothermal power plant power output is 13,865 kWe where 20.6% go for the use of the auxiliary components. With 10.18 as cycle efficiency, the hybrid specific power output is 12.13 kW/(kg/s).

The air-cooled condenser binary model has a NPV of US $2,770,609, an IRR of 11.0%, and 24 year discounted payback period.

The hybrid solar-geothermal plant is the most economical use for the project, as it generates the highest NPV of the two proposed options ($9.9 million). It also has the highest IRR and quickest payback period on investment, of 13.0% and 18 years, respectively.

REFERENCES

AfDB, 2013: *Geothermal exploration project in the Lake Assal region*. African Development Bank, Rabat, 31 pp.

Ahangar, F.A., 2012: Feasibility study of developing a binary power plant in the low-temperature geothermal field in Puga, Jammu and Kashmir, India. Report 6 in: *Geothermal training in Iceland 2012.* UNU-GTP, Iceland, 1-24.

Aquater, 1981: *Project for evaluating geothermal resources*. ISERST, Djibouti, report (in French).

Aquater., 1989: *Geothermal exploration project. Republic of Djibouti. Final Report*. ISERST, Dhibouti, 159 pp.

Awaleh, M.O., Hoch, F.B., Boschetti, T., Soubaneh, Y.D., and Egueh, N.M., 2015: The geothermal resources of the Republic of Djibouti: Geochemical study of the Lake Abhé geothermal field. *J. Geochemical Exploration, 159,* 129-147.

Aye, F.A., 2011: *Integration of renewable energy resources into the current energy politics of Djibouti*. University of Corsica, Corsica, report (in French).

Ayub, M., Mitsos, A., and Ghasemi, H., 2015: Thermo-economic analysis of a hybrid solar-binary geothermal power plant. *Energy, 87(C),* 326-335.

Bagley, M., Bryan, S., Loew, D., and Schaal, A.E., 2004: *A petrologic study of the Afar triangle basalts: is new oceanic crust forming in East Africa*. Carleton University, Ottawa, Canada.

Bandoro, R.S., and Pálson, H., 2010: Modelling and optimization of possible bottoming units for general single flash geothermal power plants. *Proceedings of the World Geothermal Congress 2010, Bali, Indonesia*, 11 pp.

Bouh, H., 2010: Geochemistry overview of hot springs from the Lake Abhe area. *Proceedings of the ARGeo-C3 conference, Djibouti, Republic of Djibouti,* 158-169.

BRGM 1980: *Report on project DJI78/005. Testing of geothermal fluids, Lac Asal, Republic of Djibouti, phase 1.* BRGM, report, 27 pp.

Cengel, Y., and Boles, M., 2006: *Thermodynamics: an engineering approach* (5th ed.). McGraw-Hill, NY, 963 pp.

Çengel, Y., and Boles, M., 2015: *Thermodynamics: an engineering approach* (8th ed.). McGraw Hill Education, NY, 1024 pp.

Climatemps, 2018: *Djibouti climate data*. Climatemps, website: *www.djibouti.climatemps.com/.*

Cosar, R., 2018: *Lake Abbe*. Wikimedia, website: *commons.wikimedia.org/wiki/Category:Lake_Abbe#/media/File:Lac_Abbe-01.JPG*

Dickson, M.H., and Fanelli, M. (eds.), 2003: *Geothermal energy. Utilization and technology*. UNESCO, Renewable Energy Series, 205 pp.

Dipippo, R., 2008: *Geothermal power plants. Principles, applications, case studies and environmental impact*. Elsevier Ltd., Kidlington, UK, 493 pp.

DISED, 2009: Second general census of the population and housing. Directorate of Statistics and Demographic Studies, Djibouti City (in French).

Gehringer, M., and Loksha, V., 2012: *Geothermal handbook: planning and financing power generation.* ESMAP, technical report 002/12, World Bank, Washington, DC.

F-Chart Software, 2016: *EES, Engineering equation solver*. F-Chart Software internet website, *www.fchart.com/ees/ees.shtml.*

Forsha, M.D., and Nichols, K.E., 2018: *Design and manufacture of special turbomachinery*. Barber and Nichols, website:
www.barber-nichols.com/sites/default/files/wysiwyg/images/factors_affecting_the_capital_cost_of_binary_power_plants.pdf

Frick, S., Kranz, S., and Saadat, A., 2015: Improving the annual net power output of geothermal binary power plants. *Proceedings of the World Geothermal Congress 2015, Melbourne, Australia*, 9 pp.

Garg, S.K., and Combs, J., 2011: A re-examination of USGS volumetric "heat in place" method. *Proceedings of the 36th Workshop on Geothermal Reservoir Engineering, Stanford University, Stanford, CA*, 5 pp.

Geothermal Energy Association, 2014: *The economic costs and benefits of geothermal power*. GEA, Washington 9 pp.

Global Volcanism Program, 2018: *Dama Ali*. Smithsonian Institution, website:
volcano.si.edu/volcano.cfm?vn=221141.

Goverment of Djibouti, 2018: *Presidential decrees.* President of the Republic of Djibouti, website: *www.presidence.dj/texte.php?ID=2016-199andID2=2016-03-22andID3=Arr%EAt%E9andID4=6andID5=2016-03-31andID6=n.*

Gradzinski, M., Wrobblewski, W., and Bella, P., 2015: Cenozoic freshwater carbonates of the Central Carpathians (Slovakia): facies, environments, hydrological control and depositional history. Guidebook, field trips accompanying 31st IAS Meeting of Sedimentology, Kraków, Chapter: B7: 26-28, Polish Geological Society, Kraków, 217–245.

Gunnlaugsson, E., Ármannsson, H., Thórhallsson, S., and Steingrímsson, B., 2014: Problems in geothermal operation scaling and corrosion. *Paper presented at Short Course VI on Utilization of Low- and Medium-enthalpy Geothermal Resources and Financial Aspects of Utilisation, Santa Tecla, El Salvador: organized by UNU-GTP and LaGeo, Santa Tecla*, 17 pp.

Hughes, R.H., and Hughes, J.S., 1992: Djibouti. In: Hughes, R.H. and Hughes, J.S. (eds.), *A directory of African wetlands.* IUCN, UNEP and WCMC, Gland, Switzerland, 130-134.

IFC, 2013: *Success of geothermal wells: A global study*. International Finance Corp., Washington DC, USA, 80 pp.

International Energy Agency, 2010: *Renewable energy essentials: Geothermal*. OECD/IEA, Paris, 4 pp.

IRENA, 2012: *Renewable energy technologies: Cost analysis series. Concentrating solar power*. IRENA, Dubai, 48 pp.

ISERST, 1984: *Potential energy sources for Djibouti*. ISERST, Djibouti, report (in French).

Jalludin, M., 2012: State of knowledge of the geothermal provinces of the Republic of Djibouti. *Papers presented at Short Course VII on Exploration for Geothermal Resources, organised by UNU-GTP, KenGen and GDC in Naivasha, Kenya,* 17 pp.

JICA, 2014: *Data collection survey on geothermal development in the Republic of* Djibouti. JICA, Djibouti.

Khaireh, A., Moussa, K., and Magareh, H., 2016: Lake Abhe geothermal prospect, Djibouti. *Proceedings of the ARGeo-C6 Conference, Addis Ababa, Ethiopia,* 16 pp.

Lonely Planet, 2018: *Map of Djibouti.* Lonely Planet, maps of the world, website: *www.lonelyplanet.com/maps/africa/djibouti/.*

Mendrinos, D., Kontoleontos, E., and Karytsas, C., 2006: Geothermal binary plants: Water or air cooled? Engine, 2nd Work Package Meeting, Strasbourg, France, 10 pp.

Moon, H., and Zarrouk, S., 2012: Efficiency of geothermal power plants: A Worldwide review. *Proceedings of the 2012 New Zealand Geothermal Workshop, Auckland , NZ*, 13 pp.

Muffler, L.P.J. (editor), 1979: *Assessment of geothermal resources of the United States - 1978.* USGS Circular 790, Arlington, VA.

Najafabadi, A., 2015: Geothermal power plant condensers in the world. *Proceedings of the World Geothermal Congress 2015, Melbourne, Australia*, 7 pp.

National Geographic, 2016: *Geothermal energy*. National Geographic, website: *www.nationalgeographic.com/environment/global-warming/geothermal-energy/*

ODDEG-ISOR, 2016: *Djibouti – Lake Abhé surface exploration studies in 2015, conceptual model.* ODDEG, Djibouti.

Pálsson, H., 2010: *Utilisation of geothermal energy for power production*. UNU-GTP, unpublished lecture notes.

Pentecost, A., and Viles, H., 1994: A review and reassessment of travertine classification. *Géographie physique et Quaternaire, 48-3,* 305-314.

Quoilin, S., Declaye, S., Tchanche, B., and Lemort, V., 2011: Thermo-economic optimization of waste heat recovery Organic Rankine Cycles. *Applied Thermal Engineering, 31*, 40 pp.

Sarmiento, Z. F., and Steingrímsson, B., 2011: Resource Assessment I. Introduction and volumetric assessment. *Paper written for "Short Course on Geothermal Drilling, Resource Development and Power Plants", organized by UNU-GTP and LaGeo in Santa Tecla, El Salvador*, 15 pp.

Shao-Qianq, S., 2015: How to generate electricity in the Republic of Djibouti? *Proceedings of the World Geothermal Congress 2015, Melbourne, Australia,* 6 pp.

Smithsonian Institution, 2018: *Alu-Dalafilla.* Smithsonian Institution, website: *volcano.si.edu/showreport.cfm?doi=10.5479/si.GVP.BGVN200810-221060:*

Souleiman C., H. 2010: Prefeasibility design of a 2×25 MW single-flash geothermal power plant in Asal, Djibouti. Report 28 in: *Geothermal training in Iceland 2010*. UNU-GTP, Iceland, 589-610.

Souleiman, H., and Moussa, A.O., 2015: Country report, geothermal development in Djibouti Republic. *Proceedings of the World Geothermal Congress 2015, Melbourne, Australia,* 5 pp.

Stacey, F., and Davis, P.M., 2008: *Physics of the earth*. Cambridge University press, NY, 13+532 pp.

Tazieff, H., Varet, J., Barberi, J., and Giglia, C., 1972: Tectonic significant of the Afar (or Danakil) depression. *Nature, 235,* 144-147.

Travel Adventures, 2018: *Djibouti: Lake Abhé.* Travel Adventures, website: *www.traveladventures.org/continents/africa/lac-abbe02.html*

US EIA, 2013: *Updated capital cost estimates for utility scale electricity generating* plants. US DoE, Washington DC, 141 pp.

VERKÍS, 2014: *Geothermal binary power plants; preliminary study of low temperature utilization cost estimates and energy cost.* Verkís Consulting Engineering, Reykjavik, report for ICEIDA - Icelandic International Development Agency.

Virkir-Orkint, 1990: *Djibouti geothermal scaling and corrosion study.* Virkir-Orkint, Reykjavik, final report, 109 pp.

Williams, C., 2007: Updated methods for estimating recovery factors for geothermal resources. *Proceedings of the 32nd Workshop on Geothermal Reservoir Engineering, Stanford University, Stanford, CA*, 7 pp.

Woodhurst, C., 2014: *Silica scaling in heat exchangers and its impact on pressure drop and performance: Wairakei binary plant.* Auckland University, Auckland, NZ.

Zhou, C., 2014: Hybridisation of solar and geothermal energy in both subcritical and supercritical ORC. *Energy Conversion and Management, 81*, 72-82.

Zhou, C., Doroodchi, E., and Moghtaderi, B., 2013: An in-depth assessment of hybrid solar-geothermal power generation. *Energy Conversion and Management, 74*, 88–101.

APPENDIX I: Map of resistivity at 100 m a.s.l. from Lake Abhé

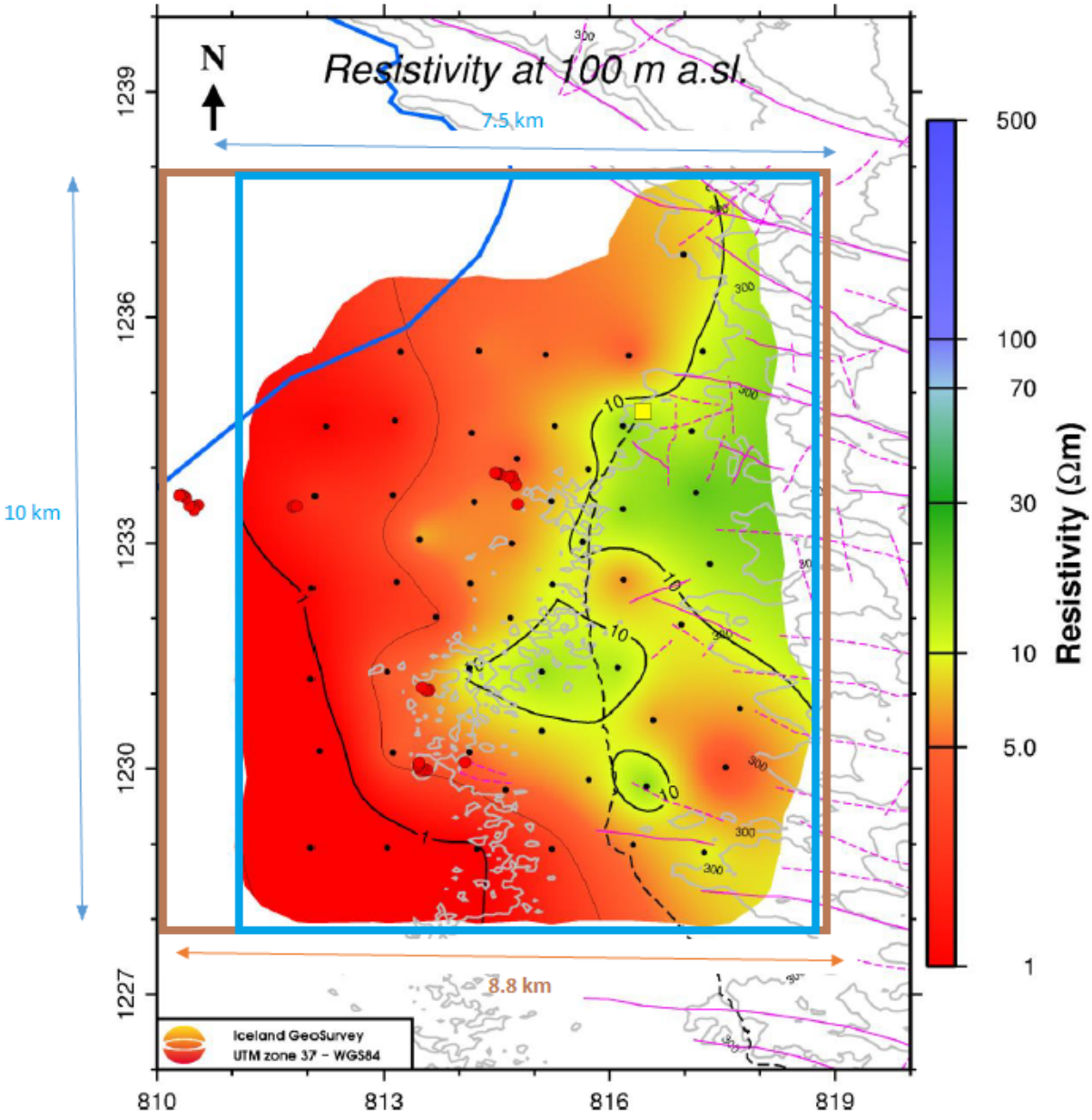

FIGURE 1: Resistivity depth slices at 100 m a.s.l. modified from (ODDEG-ISOR, 2016). Brown square is the largest field area calculated to be 88 km^2. The blue square is the most likely geothermal surface area, at 75 km^2